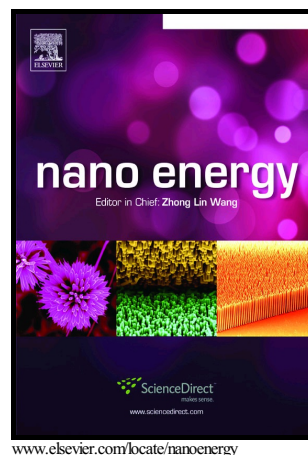


Author's Accepted Manuscript

Towards Self-Powered Sensing Using
Nanogenerators for Automotive Systems

Hassan Askari, E. Hashemi, A. Khajepour, M.B.
Khamesee, Z.L. Wang



PII: S2211-2855(18)30676-1
DOI: <https://doi.org/10.1016/j.nanoen.2018.09.032>
Reference: NANOEN3037

To appear in: *Nano Energy*

Received date: 23 July 2018
Revised date: 3 September 2018
Accepted date: 14 September 2018

Cite this article as: Hassan Askari, E. Hashemi, A. Khajepour, M.B. Khamesee and Z.L. Wang, Towards Self-Powered Sensing Using Nanogenerators for Automotive Systems, *Nano Energy*, <https://doi.org/10.1016/j.nanoen.2018.09.032>

This is a PDF file of an unedited manuscript that has been accepted for publication. As a service to our customers we are providing this early version of the manuscript. The manuscript will undergo copyediting, typesetting, and review of the resulting galley proof before it is published in its final citable form. Please note that during the production process errors may be discovered which could affect the content, and all legal disclaimers that apply to the journal pertain.

Towards Self-Powered Sensing Using Nanogenerators for Automotive Systems

Hassan Askari^a, E. Hashemi^a, A. Khajepour^a, M.B. Khamesee^a, Z. L. Wang^b

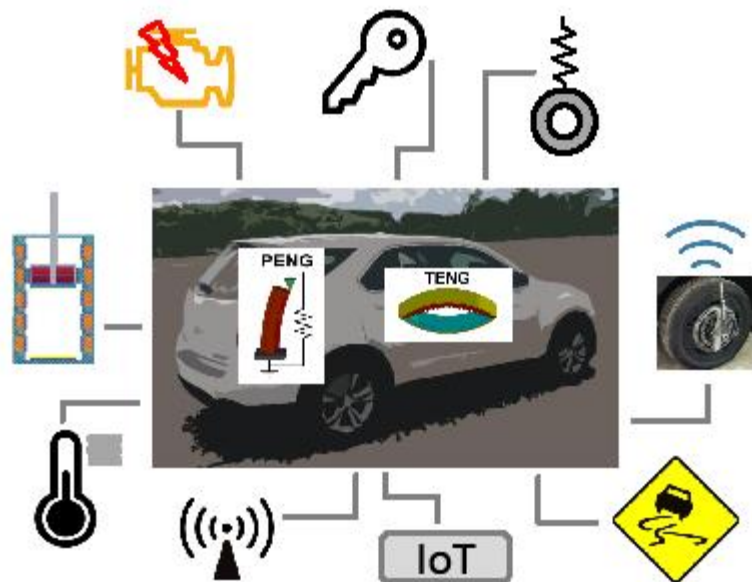
^a*Department of Mechanical and Mechatronics Engineering, University of Waterloo, 200 University Ave. West, Waterloo, ON N2L 3G1, Canada*

^b*School of Materials Science and Engineering Georgia Institute of Technology, Atlanta, GA 30332-0245, USA*

Abstract

Harvesting energy from the working environment of vehicles is important for wirelessly monitoring their operation conditions and safety. This review aims at reporting different sensory and energy harvesting technologies developed for automotive and active safety systems. A few dominant sensing and power harvesting mechanisms in automotive systems are illustrated, then, triboelectric, piezoelectric and pyroelectric nanogenerators, and their potential for utilization in automotive systems are discussed considering their high power density, flexibility, different operating modes, and cost in comparison with other mechanisms. Various ground vehicles' sensing mechanisms including position, thermal, pressure, chemical and gas composition, and pressure sensors are presented. A few novel types self-powered sensing mechanisms are presented for each of the abovementioned sensor categories using nanogenerators. The last section includes the automotive systems and subsystems, which have the potential to be used for energy harvesting, such as suspension and tires. The potential of nanogenerators for developing new self-powered sensors for automotive applications, which in the near future, will be an indispensable part of the active safety systems in production cars, is also discussed in this review article.

Graphical **Abstract:**



Keywords:

Self-powered sensing, nanogenerators, automotive systems, energy harvesting

1. Introduction

Cars will become vastly safer through new technologies in sensors, actuators, and vehicle dynamic control. A state-of-the-art vehicle has more than 100 sensors for monitoring its safety, power generation, power transmission, navigation, state estimation, and chassis control systems. The final aim of these sensors is to enhance passenger safety. These sensors are implemented in different parts of a vehicle including engine, chassis, brake, suspension, tire, driveshaft, clutch shaft, exhaust, airbags, mirrors, seats, seatbelts, and fuel tank. In this review article, a few of sensing techniques in vehicles are briefly illustrated. In addition, the potential of new techniques such as triboelectricity and nano-piezoelectricity is introduced in automotive systems. The main content of the paper is as follows:

The main objective of this review article is to provide information about the latest technology in sensing for vehicle systems and to discuss the potential of nanogenerators (NGs) for developing self-powered sensors for automotive applications. The main concept and mechanisms of nanogenerators are briefly described for sensing in automotive systems.

A few sensing and energy harvesting methods are discussed first, and then different types of sensors including position, thermal, pressure, inertial, chemical and gas composition are illustrated. Nanogenerators have shown a great potential for sensing and power harvesting applications taking into account their power density, flexibility, weight, high efficiency at low frequency, cost and diverse choice of materials. The above features of nanogenerators make them very suitable choices for automotive systems, and therefore, they can be considered as a reliable sensing and detection technologies in active safety systems with lower costs and higher accuracy. Furthermore, developing self-powered sensors for automotive systems reduces the electrical wiring in a car and also its pertinent maintenance cost. In addition, utilization of nanogenerators as power harvesting and self-powered devices in vehicles alleviates their fuel consumption, which is highly beneficial for environment in terms of reduction of CO₂ emission and concerns related to the global warming. This leads us to discuss the potential of nanogenerators for developing new types of self-powered sensors in automotive systems for each of the abovementioned sensor categories. The last part of this article provides a review on the applications of nanogenerators for developing future intelligent tires and their capability for power harvesting in suspension systems. Furthermore, plenty of potential sensors in automobile systems, which can be promoted to the category of self-powered devices using nanogenerators are presented. In fact, this work opens a new door for researchers and industries in areas of automotive systems, material sciences, mechanical engineering, intelligent transportation, self-powered sensors, energy harvesting and vehicle dynamics to focus on designing novel sensory devices using nanogenerators for automotive systems.

2. Methods

The mechanisms of sensing in automotive systems include variable reluctance, Hall-effect, anisotropic magneto-resistive (AMR), giant magnetoresistive (GMR), potentiometric, MEMS piezoresistor, fiber-optic, capacitive-based module, resistive temperature, thermistors, eddy currents, surface acoustic wave (SAW), capacitive MEMS, vibrating ring, camera on-chip

technology, solar radiation detection, infrared radiation, ultrasonic Doppler, pulsed Doppler radar, monopulse radar, laser, far-infrared (FIR), and near-infrared (NIR). Figure 1 illustrates most of the current technologies for sensing in automotive systems.

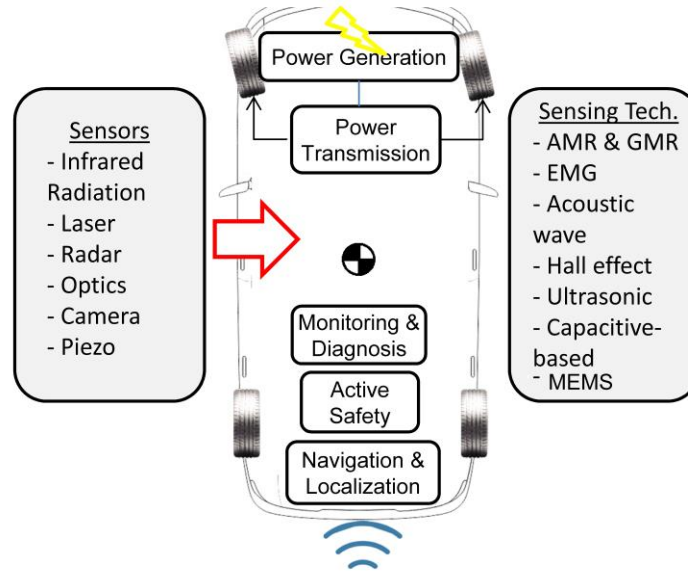


Figure 1 Current technology in automotive sensory systems.

In the next section, nanogenerators and three main sensing techniques, which are currently being utilized in vehicles and energy harvesting, are discussed.

2.1. Electromagnetism

Theory of electromagnetism, which is in fact a cornerstone of classical physics, was developed by Maxwell during 1860-1871[1]. The following equations are the basis of many different technologies varying from macro to nano systems:

$$\nabla \cdot D = \rho, \nabla \cdot B = 0, \nabla \times E = -\frac{\partial B}{\partial t}, \quad (1)$$

$$\nabla \times H = \frac{\partial D}{\partial t} + J. \quad (2)$$

where D , H , B , E , J and ρ represent electric displacement field, magnetic field strength, magnetic flux density, electric field, free current density, and free electric charge density. This set of equations are fundamental relations in Antenna, radio, TV, microwave, wireless

communications, Internet of Thing (IoT), sensors, and blue energy harvesting [2]. In automotive systems, magnetism can be found in anisotropic magneto-resistive (AMR) [3] and giant magneto resistive (GMR)[4], [5] speed/timing sensors, magnetically poled encoder rings[6], dual-magnet sensors [7], TPMS [8], torque sensors [9], seatbelt tension sensors[10], seatbelt buckle status sensor[11], and seat position sensors [12]. In the next part, the main methods in vehicle sensors based on the electromagnetism are discussed in detail.

2.1.1. Anisotropic magneto-resistive (AMR)

In 1857, W. Thomson discovered the anisotropic magnetoresistive (AMR) effect [13]. Thomson's experiment showed the dependency of resistivity of ferromagnetic materials on the angle between the direction of electric current and the orientation of magnetization. In general, magnetoresistive (MR) sensors are fabricated in different shapes with several applications such as: high density read heads for tape and disk drives, compass navigations, current sensing, vehicle detection, vehicle wheel speed, etc. AMR sensors are also used for sensing DC static fields, and field strength and direction. Generally, AMR consists of a nickel-iron thin film deposited on a silicon wafer. Due to the material properties of AMR, its resistance is altered about 2-3 % under magnetic field. Automotive applications of this technique include vehicle direction detection, vehicle classification, and identifying vehicle presence and wheel speed measurement [4], [14].

2.1.2. Hall effect

Edwin Hall discovered the Hall Effect, and reported it in a paper in 1879 [15]. The Hall effect is in fact the generation of voltage difference across an electrical conductor, which is transverse to an applied magnetic field, perpendicular to the current and an electric current in the conductor. This simple idea is the basis of several types of Hall effect sensors for different applications including automotive systems. In order to activate a Hall effect sensor, an external magnetic field is necessary. In fact, the performance of the Hall effect sensor depends on the magnetic field density adjacent to the device. If the magnetic flux density around the sensor exceeds the pre-defined threshold, it will be detected by the sensor and, as a result, the Hall effect sensor generates an output signal called Hall voltage.

2.1.3. Eddy current

François Arago, the 25th Prime Minister of France, who was also a mathematician, physicist and astronomer, observed the Eddy current for the first time. His discovery was then completed by

Michael Faraday. Owing to Faraday's law of induction, changing the magnetic field in the conductor results in loops of electrical current within conductors, which are called Eddy currents [16]. Eddy currents are utilized in electromagnetic braking system, vibration and position sensing, structural testing, etc.

2.1.4. Energy harvesting

Energy harvesting based on electromagnetism has several applications such as harvesting energy from wind, ocean wave, and wasted kinetic energy. All of the electromagnetic harvesters operate based on Faraday's law of electromagnetic induction. Thus, an electromagnetic energy harvester should be designed using at least one coil and one magnet, and relative motion between them to generate electrical power. Due to the relative motion between a coil and a magnetic field, a current flow is generated in the coil. Suspension systems and tires are considered the potential components in ground vehicles for energy harvesting based on electromagnetism.

2.2. Triboelectricity

Triboelectrification has been recently proposed for energy harvesting and active sensing purposes [17]–[19]. The triboelectric effect is basically a type of contact electrification in which specific materials become electrically charged after they come into frictional contact with a different material. Based on a conjunction of triboelectrification and electrostatic induction, triboelectric nanogenerators (TENGs), which could convert mechanical energy into electricity, are introduced [19]. TENGs exhibit a very highly efficient performance in terms of energy conversion, even under operation in variable and harsh environments [20], [21], [22]. Therefore, TENGs have been widely utilized for a variety of applications such as flexible and wearable electronics, biomedical implantable devices, vibration energy harvesting, and active sensing [2]. In addition, they can be simply fabricated with cost-effective and lightweight materials delivering high power densities for vast micro and macro scale systems [2]. Triboelectric nanogenerators have been used for plenty of different applications including traffic monitoring [23], pressure sensing [24], bioengineering, ocean wave harvesting [25], [26], wind energy harvesting [27], and other applications [28]. In addition, researchers have designed hybridized TENG-EMG self-powered sensor for human motion based energy harvesting [29], [30].

The working principle of this method is based on the premise that when two different materials are brought into contact, a chemical bond is formed between the two surfaces and then charges,

i.e. in the form of electrons or ions/molecules, move between the two materials to make the electrochemical potential equal for each material. This surface charge transfer is due to the difference between the polarities of triboelectricity for the two distinct materials; therefore, one surface achieves positive charges unlike the other surface which has negative charges. This effect causes an inner potential leading to a charge in outer layers of each material which are generally covered by electrodes. As the surfaces of the two materials are separated, the charge in the inner layers becomes unbalanced that causes a charge flow to the outer layers to maintain the balance. Therefore, as the distance of two surfaces intermittently changes, an alternative current is generated in the outer circuit, which results in electrical power generation. This alternative change of distance can be obtained by mechanical stimuli converting kinetic energy to electricity. It should be noted that the two materials must have distinct electron affinities and at least one of them must be an insulator.

2.2.1. Operating modes

Different working modes for TENGs have been recently discovered and developed based on the concept of triboelectrification. Accordingly, four main operating principles for TENGs [17], [22] are discussed in the following paragraphs. The red and blue colors in all figures of this section indicate two distinct materials with opposite electron affinities, and yellow color represents an electrode layer.

2.2.1.1. Contact-separation mode

The contact-separation mode, the system operation is schematically presented in Figure 2, is the first mode discovered for TENG. First, the two surfaces are brought into contact and then separated by a gap. The corresponding electrodes are connected to a load and consequently the electron flow is observed in the formed circuit. Periodic contact and separation of the two materials results in back and forth flow leading to an AC output. The periodic contact-separation switching plays an important role in the power generation; thus, various methods have been designed for this mode of operations such as cantilevers, spring supported systems, arch and cymbal shapes [18], [31]. One of the advantages of this method is that it can be operational in low-frequency inputs which enables it to be applied in human body kinematics, biomedical devices, machine vibrations, pressure sensors, etc. [18], [31].

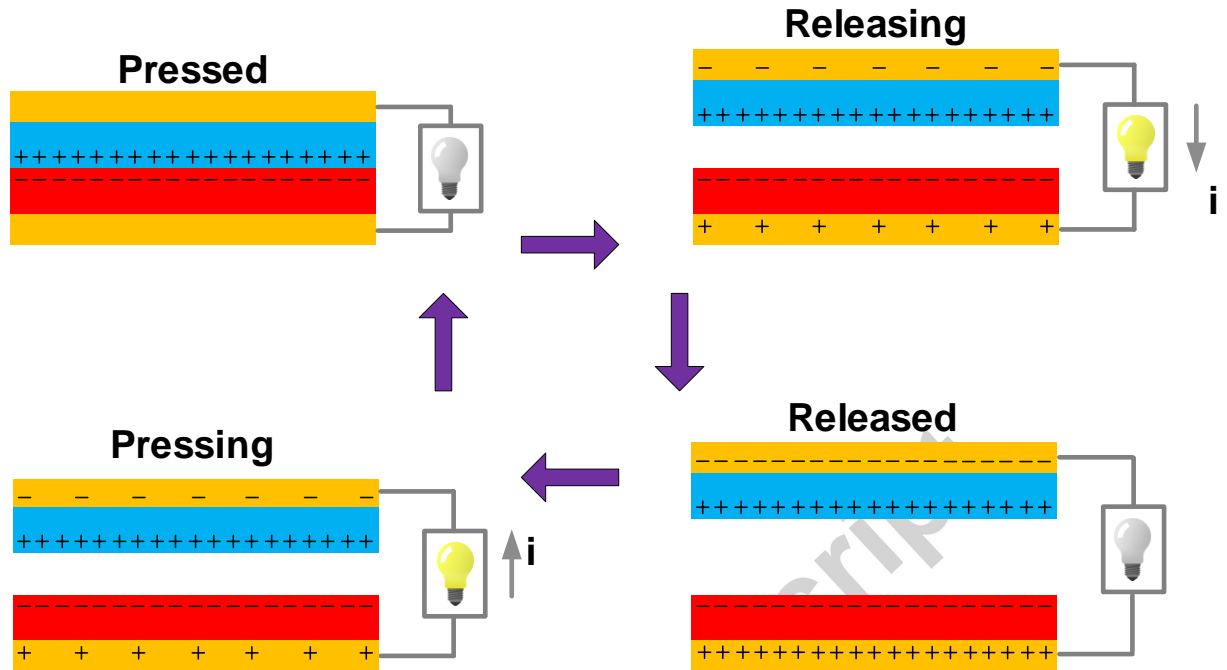


Figure 2 Contact mode TENG [32].

2.2.1.2. Sliding mode

This working mode is based on the relative sliding motion between the two triboelectric surfaces, as depicted in Figure 3. This type of motion causes potential differences across the two materials, which can result in charge flow in outer electrodes. The sliding motion of the two surfaces, originated from the alternative external forces, is more efficient than the first mode in order to improve the output power, which can be harnessed by the external electrical circuits. Also, this mode can be operated in a variety of ambient motions such as linear and rotational systems which can be easily implemented in wind and ocean energy harvesting as well as motion sensors [18], [31]. High-frequency sliding motion is required for this mode to reach the desired output power for the system.

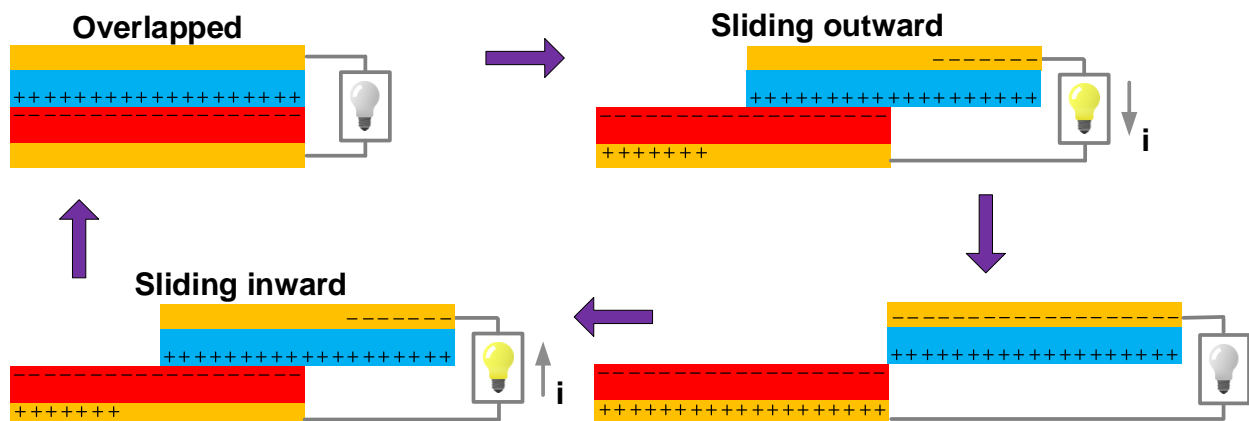


Figure 3 Sliding mode TENG[33].

2.2.1.3. Single-electrode mode

One of the interesting and simple configurations of TENG is known as the single-electrode mode, as shown in Figure 4. The tribomaterial (such as a polymer) is the moving object, while the other material (such as a metal electrode) is fixed and electrically connected to the ground. The working principle of this mode is based on the electron flow between the electrode layer and the ground which is a result of the unbalanced charge between the moving and fixed layers. This unbalanced charge can be obtained by having contact/sliding and separation of the polymer and the electrode. The outstanding feature of this simple structure is that one of the layers is not bounded in motion and therefore can be used for various mechanical, chemical, and biomedical self-powered sensors [18], [31]. It is worth noting that an electrostatic screening effect appears in the system operation, thus reducing the electrode induction, which is known as an important drawback of this mode and may restrict its use for some specific applications.

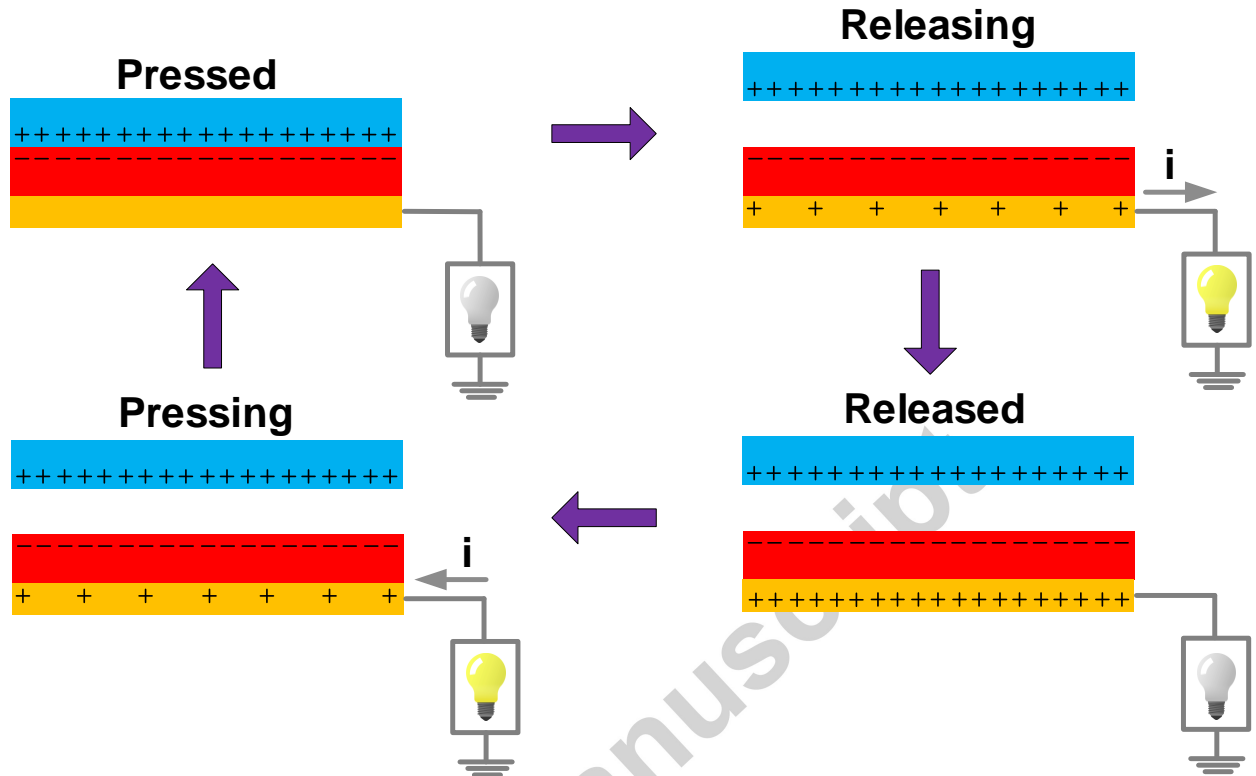


Figure 4 Single-electrode mode TENG[34].

2.2.1.4. Free-standing mode

The free-standing mode is mainly used to eliminate the need of attached electrodes in the structure, as seen in Figure 5. In this mode, a pair of symmetrical metal layers are located in a line with a small gap and the moving dielectric, which has the same length of the fixed layers, is moving above the two layers. The oscillation of this layer between the two metals leads to asymmetric charge distribution, thus, an electrical flow is generated in the external circuit. This mode has shown a longer operation life-time in comparison with the second mode due to its lower material abrasion and heat generation, as well as high energy efficiency. These features enable this mode to be used for various energy harvesting applications such as human motion measurement, automotive systems, air flow measurement, and diverse self-powered sensors [18], [31].

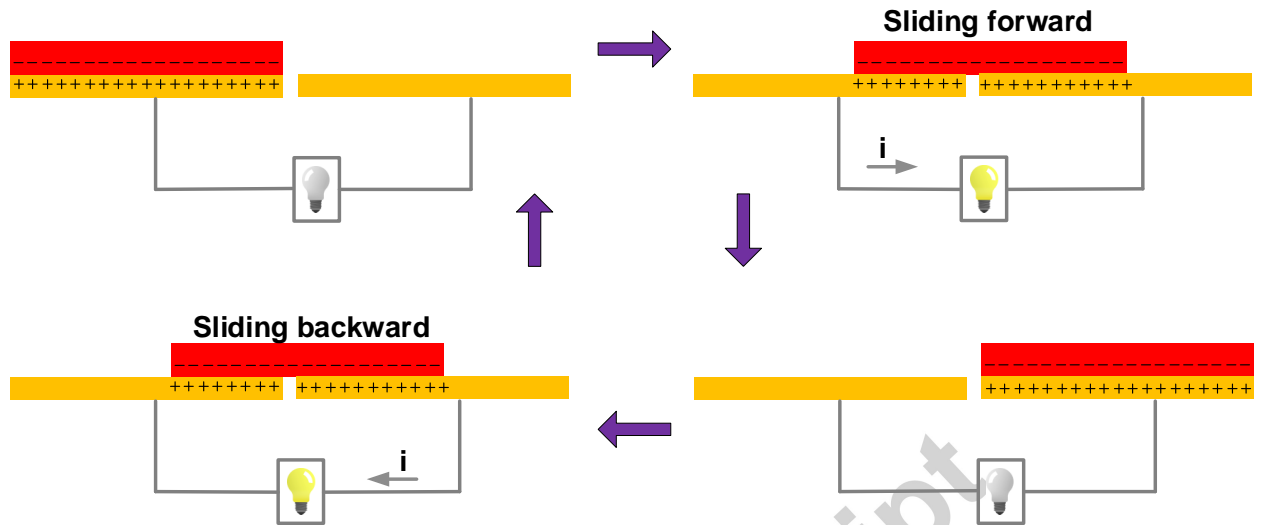


Figure 5 Free-standing sliding modes TENG.

2.3. Piezoelectricity

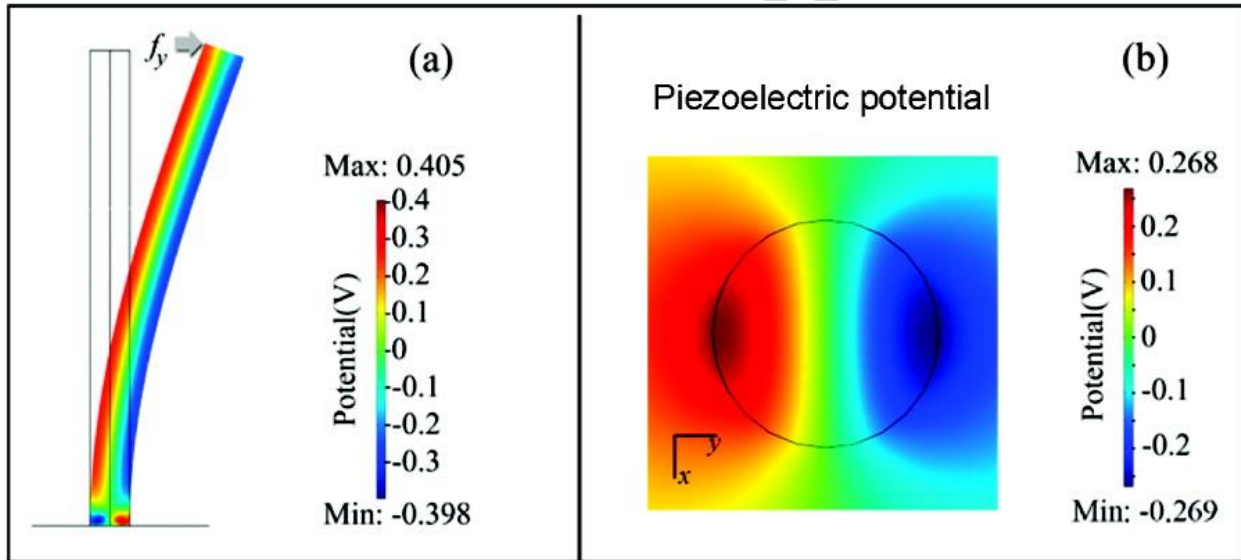
Piezoelectricity is another common technique with applications in both sensing and energy harvesting. The ability to convert applied strain energy into electrical output in piezoelectric materials has attracted the attention of numerous of researchers to implement them in both energy harvesting and sensing applications. In addition, piezoelectric materials can be easily integrated into a system. This makes them a suitable choice for implementation in different devices, which require a sustainable power source. The electrical output is generated in piezoelectric materials because of the orientation of their molecular structure. This molecular structure results in a local charge separation, which is called an electric dipole. Accordingly, when a mechanical load is applied to piezoelectric materials, a deformation of dipole occurs, which results in the formation of an electrical charge. This electrical charge can be removed from the piezoelectric materials to be used in sensing and power generation.

Zirconate Titanate, a piezoelectric ceramic (piezoceramic), known as PZT is the most common type of piezoelectric materials with applications in power harvesting. Although PZT has been used for power harvesting, it is highly brittle, which limits the applied strain to this type of piezoelectric materials. There are a few other piezoelectric-based materials with applications in sensing and power harvesting such as poly (vinylidene fluoride) (PVDF), piezofiber, flexible piezoelectric materials, MFC composite and piezoelectric nanogenerators.

2.3. 1. Piezoelectric Nanogenerators

Piezoelectric ZnO nanowires (NWs) were first proposed by Z.L. Wang at the Georgia Institute of Technology as a new platform for energy harvesting and sensing [35]. This concept has shown a remarkable potential for harvesting wasted kinetic energy from micro and nano-scale mechanical devices. The electrical output generation of ZnO nanowires under a mechanical deflection is caused by the piezoelectric potential generation on the side surfaces because of crystal lattice distortion. Basically, when a piezoelectric NW goes under deflection, the side under tensile gives a positive potential and the other side, which is under compressive load, gives a negative potential. Figure 6 shows potential distribution for a ZnO NW [36].

Figure 6 Potential distributions for a ZnO NW. (a) Side view of the potential profile. (b) Cross-sectional view of the piezoelectric potential; reprinted with permission [37], Copyright 2006 Science.



Implementation of NWs provides three exceptional advantages: i) high sensitivity to small forces, ii) superior mechanical properties, and iii) enhanced piezoelectric effects. These three unique features make them suitable for plenty of sensing and energy harvesting applications. In order to better explain the working mechanism of nanogenerators fabricated from piezoelectric

semiconductors materials, the coupled semiconducting and piezoelectric properties [36] could be studied. It must be noted that the direction of the exerted force on piezoelectric materials affects the power generation of piezoelectric nanomaterials. These materials can be used for both AC and DC electric generation [38], [39].

When a perpendicular external force is applied to vertically grown piezoelectric semiconducting NWs, stacked between the bottom and top electrodes, AC power is generated [33]. In order to generate a DC power in NWs, a force perpendicular to the axis of semiconducting NW must be applied. This applied force leads to a lateral bending in NW. For example, when an external force is applied using a moving tip, deformation occurs all over the NW; resulting in generation of piezoelectric potential in NW. This piezoelectric potential generation occurs due to the relative displacement of the cations with respect to anions. Accordingly, a positive electrical potential is observed on the stretched part of NW, while a negative potential is generated at its compressed part [33].

Piezoelectric nanogenerators have been used in plenty of devices including gas sensors [40], ultrasonic wave nanogenerator [41], touch sensors and artificial skins [42], sound-driven nanogenerator [43], [44]; pressure sensing [45], a textile fiber based NG for vibration/friction energy harvesting [46], respiration-based energy harvesting [43], driving a small liquid crystal display [47], biosystems, etc.

2.4. Pyroelectricity

An abundant source of energy is wasted heat. A large amount of everyday generated energy is lost in the form of wasted heat. Altering wasted thermal energy to electricity is a challenging task [48]–[50]. Pyroelectric nanogenerators (PYNGs), were first proposed in 2012, and present a technology to scavenge energy from a time-dependent temperature variation. In 2012, Wang's group at the Georgia Institute of Technology [51], proposed pyroelectric ZnO nanowire arrays for converting heat energy into electricity. PYNGs implement the coupling of the pyroelectric and semiconducting properties in ZnO. The time-dependent variation of temperature causes a polarization electric field and charge separation along the ZnO nanowire. In fact, the time-dependent temperature fluctuation results in the variation in spontaneous polarization of a PZT thin film, and thus electron flows in external circuit. In the same year, they presented that

PYNGs have the capability of powering wireless sensors. Results of their work show that a temperature change of 45 K at a rate of 0.2 K/s results in 22 V open circuit voltage and 171 nA/cm² short circuit current density [52]. PYNGs have shown a high potential to be used as a self-powered temperature sensor with high sensitivity to small temperature changes [53]. This interesting feature of PYNGs makes them a suitable candidate for designing new types of self-powered temperature sensors for automotive applications. Section 3.3 of the present review article covers temperature sensors in vehicle systems, and briefly discusses the potential of implementing PYNGs for implementing in different parts of vehicles.

3. Sensing Systems in a Vehicle

In this section, different types of sensors used in ground vehicles are discussed. Figure 7 categorizes various types of sensors with applications in automotive systems. In this review article, we only focus on pressure, position, inertial, thermal, gas, and chemical composition sensors. Afterwards, we will discuss the potential of nanogenerators for implementation in vehicle sensory systems.

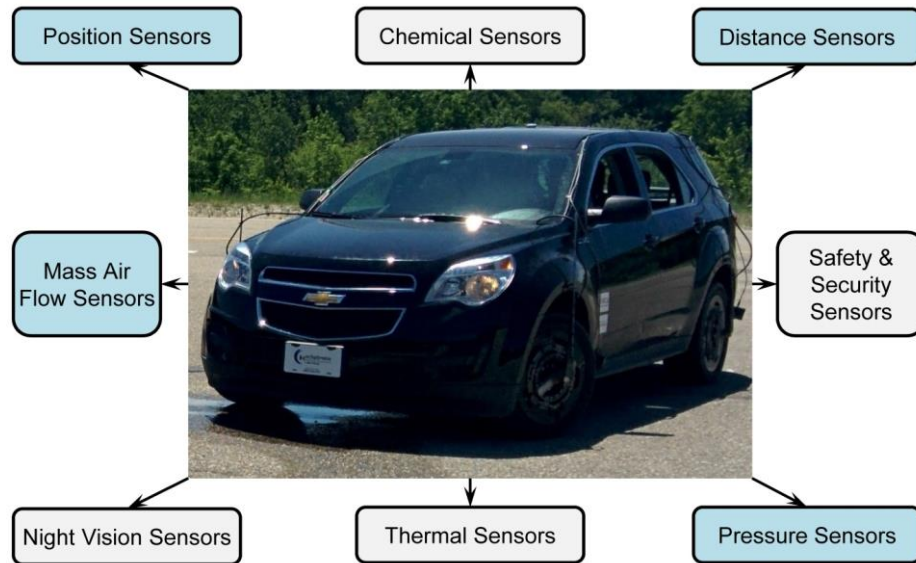


Figure 7 Different sensor categories in automotive systems

3.1. Position sensors

In order to measure rotational and linear displacements in vehicles in micro to centimeter scales, many position sensors are used. This large range of position sensing covers small motions inside of a MEMS sensor to large motion of a strut in an active suspension system. There are five different approaches for position sensing in automotive systems: Potentiometric, Hall Effect, AMR, Optical Encoder, and Magnetostrictive Pulse Transit Time (MPTT). These mechanisms have been used in various position sensors such as Fuel Level Sensor (FLS), Steering Wheel Position Sensor (SWPS), Chassis Height Sensor (CHS), Engine Throttle Position Sensor (ETPS), and Crankshaft Position Sensor (CPS).

3.1.1. Fuel Level Sensor (FLS)

There are many different approaches for fuel level sensing including capacitive, pressure-sensing, ultrasonic, radiation-absorption, and electrical-conductivity [54]. In vehicles, these sensors need to work in a harsh environment and high temperature. Changes in liquid level result in variation in level sensors' parameters, which are converted into electrical signals using an appropriate transducer. The dominant working mechanism in developing FLS is the variation of capacitance that alters based on a change in position, or properties of a dielectric material due to a level change into an electrical output [55]. Table 1 briefly describes a few research works on FLS.

Table 1 Developed fuel level sensors and methodologies

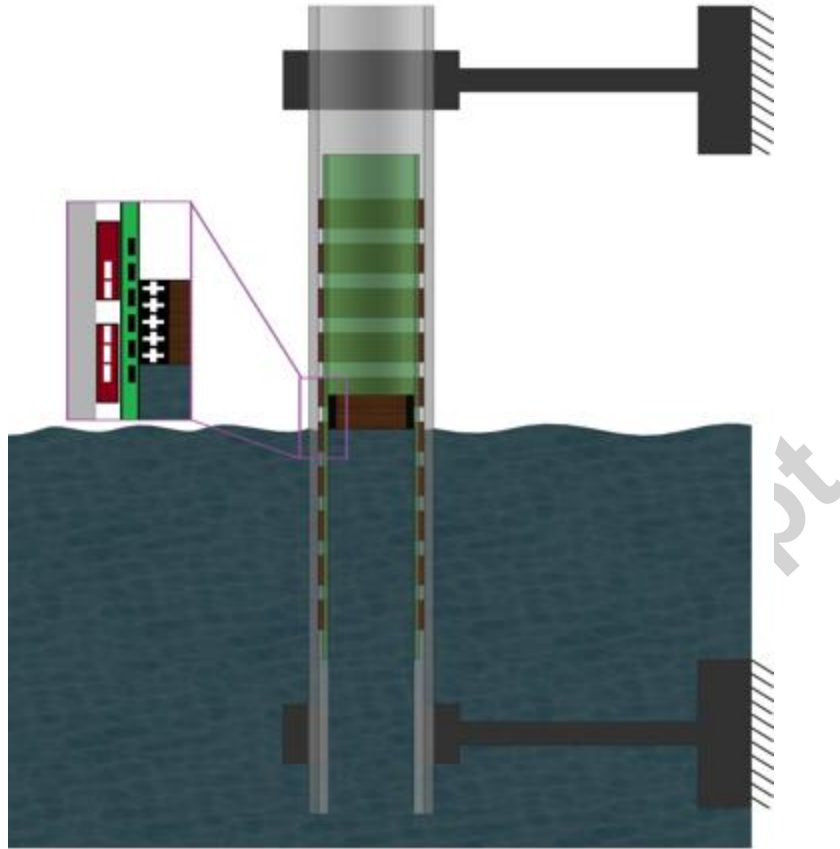
Authors	Method
Menon et al.	Designed a pneumatic capacitor and fluid amplifier feedback oscillator sensitive to liquid level [56].
Bera et al.	Developed a noncontact capacitance-type level transducer for conductive liquids[57].
Li et al.	Used the fringe effect between a high-potential surface and a low-potential surface to measure liquid level[58].
Betta et al.	Implemented an optical fiber liquid-level transducer [59].
Yun et al.	Utilized etched fiber Bragg grating to measure liquid level[60].
	Employed a guided acoustic wave through a

Royer et al.

magnetostrictive wire [61].

Table 1 covers most of the approaches for this application; however, it does not provide a complete list of fluid level sensors. As mentioned in Section 2, NGs have a high potential in vehicle sensing systems and specifically in fluid level sensing. More specifically, TENGs have not been used for fuel level sensing, but they have the potential to be implemented for this application using a sliding single electrode mode. Recently, research works have been published to show the potential of fluid-solid interaction (FSI) for energy harvesting, not for fluid level sensing applications [62], [63]. Choi et al. developed a super hydrophobic nanostructured aluminum tube to estimate electrical output for solid–water contact electrification inside a tubular system [62]. On the other hand, Zhu et al. used asymmetric screening of electrostatic charges on a nanostructured hydrophobic thin-film surface for water wave energy harvesting [63]. A conceptual design for the utilization of TENGs in fluid level sensing is proposed in this section (see Figure 8). A reliable design based on TENGs for a fluid level sensor could lead to a device, capable of working in a harsh environment. It should be highlighted that for a real world application, the internal TENG sensing chamber should be isolated from the fuel chamber to avoid potential risks of the tribo-charges and any potential hazard. Working on the designs and types of insulation parts and materials is a new research avenue that could be addressed by material and mechanical engineers.

Figure 8 A triboelectric based fluid level sensor (conceptual design)



3.1.2. Engine throttle position sensor

The engine throttle position sensor (ETPS) plays a key role in automotive powertrain systems and is used to monitor the position of the throttle valve in internal combustion engines. ETPS is usually located on the throttle valve spindle, which helps to directly monitor the position. ETPS measured data is used in the engine control module (ECM) to determine the engine mode, air-fuel ratio correction, power increase correction, and also fuel-cut control. ETPS is mechanically connected with the accelerator pedal and is actuated when the driver pushes the accelerator pedal. This sensor is basically a potentiometer with a variable resistance based on the position of the throttle valve. At the idle condition, the voltage on the signal wire is in the range of 0.6-0.9 [V]. At wide open throttle, the voltage is approximately 3.5-4.7 [V]. Triboelectric nanogenerators have a remarkable potential to be used for this application; thus, a TENG based throttle position sensor, sensitive to rotating motion of the throttle, can be designed using single electrode grating structure.

3.1.3. Steering wheel position sensor

Steering wheel position sensors (SWPS) are usually a variable position resistor [64] and are used to measure the position of the steering wheel directly; optical encoders are also implemented for this application. A combination of these two mechanisms has been implemented in vehicles' electronic stability programs (ESP) to accurately measure the position of the steering wheel. This combination not only allows incremental angular position change during steering wheel movement, thus, providing quadrature outputs to determine the direction of steer, but also provides an analog signal of the steering wheel position at any point over the 'lock-to-lock' range [65]. As an example, we can refer to a slotted-aperture optical-encoder sensor, which has been added to a gear-reduction-driven potentiometric sensor. Magnetic-based sensors can also be implemented for steering wheel position sensing. A sensor, called LWS3, developed at Robert Bosch GmbH is an example of this technology (AMR electromagnetic concept) that has been fabricated for ESP [4].

3.1.4. Chassis height sensor

Chassis Height Sensors (CHS) are another application of position sensing in vehicles' active safety, active suspension, state estimation, road angle estimation, and self-leveling headlamp systems [66]. CHS implements an angular position measurement to detect suspension's vertical movement by using the Hall effect.

3.2. Pressure Sensors

Pressure sensors are used in different parts of a vehicle such as tire, chassis, brake fluid, cylinder, exhaust, AC compressor, evaporative fuel, fuel injection, and chassis adaptive suspension monitoring systems. In this review article, we mainly focus on three pressure sensing systems in vehicles: tire pressure monitoring system (TPMS), engine manifold pressure sensing system (EMPS), and cylinder pressure sensor (CPS). Other types of pressure sensors in automotive systems include evaporative fuel pressure sensing system, brake fluid pressure sensor, exhaust pressure sensor, and fuel injection pressure sensor.

3.2.1. Tire pressure monitoring system

An active area of research in sensing and energy harvesting systems is tire pressure monitoring systems. Recent works focus on developing self-powered sensors for tire pressure monitoring systems, measuring tire forces and moments, and determining road friction conditions.

Beginning September 2007, the Federal Motor Vehicle Safety Standard (FMVSS) mandated all vehicles less than 10,000 pounds sold in the US to be equipped with tire pressure monitoring systems. Lower tire pressure (compared to vehicle manufacturer's recommendation) results in high heat generation, which can cause tire blowout, rapid tire wear, and eventually, losing vehicle lateral and longitudinal control. The use of TPMS results in longer tire life, better vehicle handling and stability, and also reducing the fuel consumption [67] by diagnosing deviations from the standard inflation pressure. In order to report the real-time tire pressure information to the driver, different types of displaying systems are used such as a gauge, pictogram, and warning light.

Tire pressure monitoring systems fall into two main categories: direct and indirect measurement systems. In an indirect tire pressure monitoring system (ITPMS), the pressure inside the tire is not directly measured and it is identified using wheel rotational speeds and other active safety system's signals available outside a tire. The first generation of ITPMS works based on a slightly lower tire diameter, and therefore, slightly higher angular velocity for under-inflated tires. In order to detect a low tire pressure, ITPMS compares the relative wheel speeds, provided by the Anti-lock Brake System (ABS) sensors, and sends a signal to the vehicle diagnosis system to actuate the indicator light when the allowable difference passes a threshold. Comparing to the direct tire pressure monitoring system (DTPMS), ITPMS is cheaper, requires less programming and also has a lower maintenance cost. ITPMS may result in faulty diagnosis, when a bigger or smaller tire is used. Such diagnosis could also be unreliable when all tires have lower pressure or are unevenly worn. They must be reinitialized after properly inflating each tire and after routine tire rotation.

DTPMS specifically measures the pressure of each tire rather than monitoring the wheels' rotational speed; this provides online information about the pressure of each tire. Usually, DTPMS sends the extracted data from tires to the vehicle active safety control and diagnosis system to evaluate and interpret the data, and warns the driver if the tire pressure is lower than

the permissible threshold. Each DTPMS has a wireless module and specific serial number for security reasons. DTPMS is more accurate than IDTPM and provides the actual pressure data. Many researchers have focused on TPMS considering different aspects such as sensing capability, energy harvesting, and network security concerns.

One important concern related to TPMS and its wireless module is pertinent to the static unique identifier, which might be used improperly and, therefore, raises concerns regarding privacy and spoofing[68], [69]. External devices other than the vehicle's central computer have the potential to receive and decode the signal from wireless TPMS. The main concern is not the status of information transmitted by a TPMS, but the data's unique identifier, which can be exploited for vehicle tracking and data mining [68], [70]–[73]. This data can be implemented for traffic purpose management[70] but could also be stolen by an eavesdropper (a static observer or on adjacent vehicles) [68]. It is an important and open challenge that needs to be addressed by telecommunication researchers to avoid security issues in vehicle systems. Section 4.1 provides information related to the energy harvesting and sensing devices in tires.

3.2.2. Engine manifold pressure sensing system

Engine manifold pressure sensing systems are used in fuel injected engines to monitor the combustion process by calculating air density and consequently determining air mass flow rate. This determines the required fuel delivery for high-performance combustion. It is also essential to sense the manifold absolute pressure for the engines' electronic control unit (ECU) to diagnose spark and fuel-ratio conditions. EMPS measures absolute pressure in the engine's intake manifold [74] using a MEMS-type or piezoresistive sensor [75].

3.2.3. Cylinder pressure sensor

To evaluate the fuel quality and environmental conditions, combustion control systems use cylinder pressure sensors (CPS), which were first developed by the Nissan Motor Co. for use on domestic models, in 1986 [76]. Cylinder pressure sensors provide essential diagnosis data in internal combustion engines such as: knocking, combustion pressure, weak combustion, air-fuel ratio, bulk average temperature of the air-fuel charge, and misfire detection [77]. Although such pressure sensors are expensive, a number of engine sensors including knock sensor and air-mass meter sensor can be replaced by a CPS[78], [79].

CPS and the capabilities of microprocessors lead to new approaches to use fundamental engine parameters for monitoring and controlling the engine. As stated above, CPS has plenty of applications in spark control technique, air-fuel ratio, bulk average temperature of the air-fuel charge, and misfire detection. In fact, CPS is the most essential sensor for detection of misfire [77]. In Table 2, applications of CPS and its advantages are briefly discussed.

Table 2 Applications of CPS in a Vehicle

Applications	Illustration
Spark Control	<p>CPS relies on feedback for spark control, and its implementation reduces the amount of required calibration for the design of each engine. In addition, it significantly improves efficiency as well as power [80]. Peak pressure concept, peak pressure feedback implementation, and closed loop control of detonation are a few of methods used for spark control based on CPS data.</p>
Fuel Air Ratio Control (FARC)	<p>FARC is critical in order to have a better transient fuel control, efficiency and emission control. The pressure time history shape is a key parameter to practical application of CPS in FARC [80]. Different methods have been developed for this application including moment descriptors, molecular weight ratio, estimation performance, combustion duration and differential equation model of pressure [81]–[86].</p>
Acoustic Resonance	<p>The combustion chamber of an engine is in fact a cavity, which has resonant frequencies. The resonant frequencies can be estimated through the measurement of CPS as reported in Ref. [80].</p>
Misfire Detection	<p>CPS measurement at two different crank angles can lead to a pressure ratio between these two angles, which can be used as direct sign of whether any combustion has occurred up to the point of the second pressure measurement. Therefore, if we define a “misfire” for cycles with late combustion, the second measured pressure must be consequently adjusted. One important issue of CPS is its thermal sensitivity, which should be considered in the CPS design considering this application [87].</p>

3.3. Thermal Sensors

Different types of thermal sensors for automotive systems are introduced and briefly discussed in this section. Vehicles thermal management systems are significant in terms of fuel economy and reliable performance [88]. Thermal sensors are used for measuring the temperature in different vehicle parts and systems including the cylinder head, battery, evaporator, fuel/water/oil lines, exhaust, cabin, and atmosphere temperatures. All of these measurements are critical to prevent any damage to the abovementioned specific parts and, consequently the passengers' safety. Two types of thermal sensors are discussed in this section: exhaust gas and engine coolant temperature sensors.

3.3.1. Exhaust gas temperature sensor

An exhaust gas temperature sensor (EGTS) is usually installed in front of the Diesel Oxidation Catalyst (DOC) or Diesel Particulate Filter (DPF). This sensor detects exhaust gas temperature and converts it into voltage. This voltage is transmitted to the ECU to control engine conditions, reduce emission, detect knock, and increase fuel efficiency. The gas temperature sensor is essential to detect engine knocks as it decreases considerably when the engine goes into a knock [89]. EGTS consists of a stainless cover to protect the thermistor and wires; sheath pin to hold the stainless wire rigidly; stainless wire to carry the thermistor signal; and a thermistor to detect temperature variation. Nanogenerators have a great potential to be used with EGTS as self-powered pyroelectric nanogenerators [51], [53], [90], which are capable of not only converting the thermal variation in the exhaust line to electrical voltage, but also providing sufficient power for signal transfer to ECU. Montaron designed a fast response, thick film nickel temperature sensing element in [91], which can be implemented by custom designing for different parts of a vehicle to act as temperature sensors such as the engine inlet air temperature, engine coolant temperature, engine oil temperature, etc.

3.3.2. Engine coolant temperature sensor

This sensor is installed in a water jacket surrounding the engine cylinders and is implemented to monitor the temperature of the internal combustion engines' coolant and consequently to adjust the fuel injection and ignition timing. Engine coolant temperature sensor data is also used to control spark advance and exhaust gas recirculation [92]. Kenny et al. [93], [94] reported one of the earliest attempts to measure coolant temperature by using a thermostat system and showed

that it is possible to maintain engine temperature at a predefined level or adjust it. The advantage of their developed system is the capability to modify engine temperature during cruise, city driving or heavy load conditions- thus, optimizing fuel economy, engine torque generation, and emissions. Another option for the engine coolant system is thermistors, which provide plenty of advantages for engine coolant system controls. This type of thermal sensor has a high durability over a million temperature cycles and does not exhibit hysteresis [95].

Furthermore, few researchers have developed a back-up system for the engine coolant temperature sensor to allow the engine to operate even if the abovementioned sensor fails [96]. A critical issue with the conventional measurement method is that if the coolant is lost, it would not be detected by the temperature coolant sensor. Accordingly, a device has been developed by Ford Global technologies (see [97]) to avoid the above mentioned circumstance to determine both temperature and presence of the coolant. Similar to EGTS, an ideal alternative for coolant temperature sensors can be a pyroelectric nanogenerator, which is thermally and mechanically durable, capable of working in harsh environments, provides the required power for sending the signal to the ECU (by wireless technology), and can be installed in the engine coolant paths.

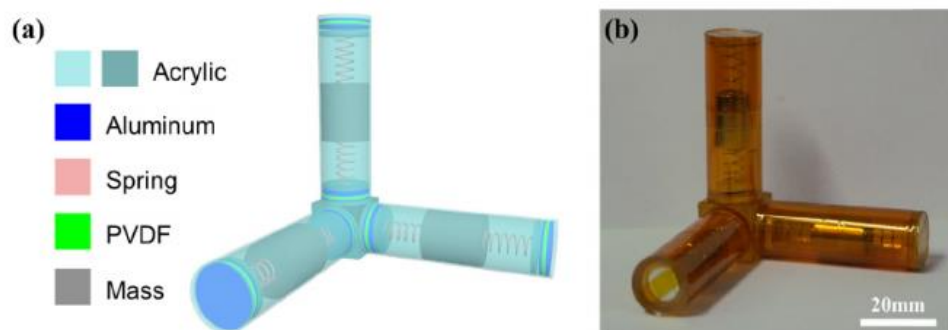
3.4. Inertial Measurement Unit

Advances in inertial sensor technologies, sensor fusion, and distributed estimation in driver-less and intelligent transportation systems facilitate reliable and robust control and estimation of vehicle states [98]–[100]. In this direction, reliable estimation of vehicle states and navigation by using an Inertial Measurement Unit (IMU) at a reasonable cost is necessary for proper functioning of active safety and driver assistance systems. Vehicle state estimators use acceleration and yaw rate measurements from an IMU and estimates the vehicle states employing Kalman-based or nonlinear observers [101]–[103], augmented systems by GPS data [104]–[107], and robust observers independent from the road friction conditions[108].

An IMU consists of accelerometers and gyroscopes to measure accelerations and angular rates. IMUs are widely used in the automotive industry for active safety, intelligent transportation, and autonomous driving systems to estimate vehicle states and road condition, control vehicle dynamics, enable anti-lock braking system (ABS), activate airbags, navigate vehicles, diagnose faults, etc [109]–[117]. IMU-enabled GPS systems also correct the measured velocity and

position data when GPS signals are unavailable due to urban canyon, tunnels, packet drop, and interference. IMUs are categorized based on their bandwidth, linearity, sample rate, and drift [118], [119]. In order to reduce the size and cost of inertial sensors for automotive applications, conventional stock IMU for active safety systems have two horizontal accelerometers and one vertical gyro [120]–[125] (so called reduced-IMU, RIMU). The pitch and roll (and their rates) cannot be measured directly from the inertial data in reduced IMUs. A gyroscope-free IMU has been developed in [126] that only includes linear accelerometers to directly measure transversal accelerations, angular accelerations, and velocities. An RIMU mechanization is investigated and evaluated with vehicle test data in [127]. Calibration of inter-triad misalignment between the gyroscope and accelerometer triads is discussed and an optimal calibration method is designed in [128]. A wireless micro IMU with a three-axis accelerometer, a three-axis gyroscope, and a three-axis magnetometer is designed [119] and its performance is demonstrated experimentally for localization. As we illustrated above, an IMU unit contains accelerometer and gyroscope to accurately measure the acceleration and relevant angular rates. Very recently, a piezoelectric nanogenerator based accelerometer was developed by Jin et al. [129] with a very high sensitivity and durability. They showed that the device has the potential to measure 3D acceleration, and can be used for vehicle dynamics monitoring. Result of this research shows the high potential of nanogenerators for implementation in IMU unit of the vehicles as self-powered accelerometers. Figure 9 shows the developed accelerometer.

Figure 9 Structure of the self-powered 3D acceleration sensor, (a) schematic of the sensor, (b) photograph of the fabricated sensor, reprinted with permission [129]; Copyright 2018 Elsevier



3.5. Gas and Chemical Compositions Sensors

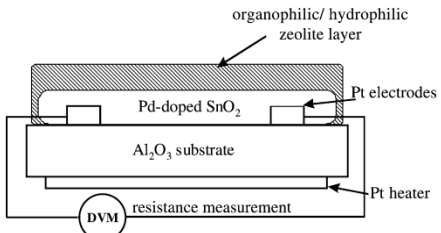
Gas and chemical composition sensors are the last sensors that are reviewed in this article. These sensors are used for monitoring ground vehicle systems that decrease harmful gas emissions that deteriorate air quality, have destructive impacts on environment, and considerably contribute to global warming. These sensors are implemented not only to monitor and reduce emissions, but also to enhance fuel efficiency by reducing unburnt fuels and improving combustion.

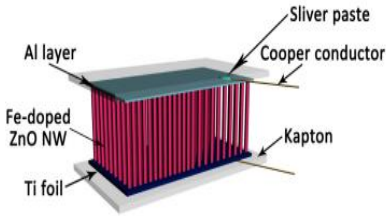
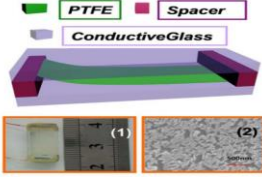
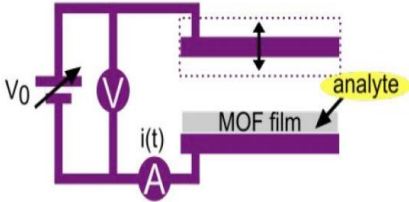
Incomplete engine combustion might result in undesired and toxic by-products such as carbon monoxide, oxides of nitrogen, sulfur dioxide, and other types of unburnt hydrocarbons. Many different types of sensors have been developed for exhaust sensing to detect humidity, NO_x , Oxygen, CO and CO_2 , Hydrocarbon, NH_3 , SO_2 , and H_2 .

3.5.1. Humidity detection sensor

Several devices have been designed and manufactured to detect humidity and concentration of water vapor, which is highly important for analyzing the extent of engine combustion and also air quality in a car cabin. Humidity sensors can be found in different parts of a vehicle to optimally regulate air inside the vehicle using air conditioning or climate-controlled seats. In addition, they are used to eliminate fogging of the windshields, ensuring a clear view of the road. In Table 3, a few of these ideas and devices are reported, which have the potential to be implemented in vehicles.

Table 3 Working principles and devices for humidity sensing

Sensor Concept	Example
<p>Zeolite-based humidity sensors: Some examples of these humidity sensors are: semiconductor sensor (Pd-doped SnO_2) covered by zeolitic films [130], a type of composite materials based on LiCl/NaY was developed by scattering of LiCl into the pores of NaY zeolite[131], Zeolite-coated interdigital capacitors[132], nanostructured Ag-zeolite composites[133], and $\text{AlPO}_4\text{-5}$ zeolite with high responsivity[134].</p>	 <p>Modified Pd-doped SnO_2 sensor scheme, where DVM is the digital voltmeter, reprinted with permission[130]; Copyright 2003 Elsevier.</p>

<p>Piezoelectric nanowire humidity based sensors: A few examples of PENG-based humidity sensor include Core-shell $\text{In}_2\text{O}_3/\text{ZnO}$ nanoarray nanogenerator as a self-powered active sensor with high H_2O sensitivity[135], Cd-ZnO nanowire nanogenerator for humidity sensing[136], Al-ZnO nanowire nanogenerator as a self-powered humidity sensor[137], Ga-doped ZnO nanowire nanogenerator [138], and Fe-doped ZnO nanoarray nanogenerator [139].</p>	 <p>The final device structure of the self-powered Fe-doped ZnO NW arrays humidity sensor, reprinted with permission [139]; Copyright 2015 Elsevier.</p>
<p>Triboelectric nanogenerator-based humidity sensors: TENG with interdigital electrodes (IDEs) as self-powered triboelectric humidity sensor (THS)[140], and airflow-induced triboelectric nanogenerator for detection of airflow and humidity[141].</p>	 <p>THS based on TENG, reprinted with permission [141]; copyright American Chemical Society 2014.</p>
<p>MOF-based humidity sensors: Some examples of these types of sensors are: Lanthanide ion MOFs humidity sensor[142], interdigital electrode impedance sensors covered by MOF thin films[143], mesoporous MOF humidity detector[144], photonic film of a MOF[145], and impedance-based MOF humidity detector.</p>	 <p>Kelvin probe setup, reprinted with permission [146]; copyright Royal Society of Chemistry 2016, Open Access.</p>

Although the majority of current humidity monitoring systems in vehicles use capacitance-based sensors (which show the variation of capacitance versus changes in relative humidity), as can be seen from Table 3, nanogenerators have the potential to be used as humidity sensors because of their self-powered sensing capability.

3.5.2. NO_x detection sensor

In order to actively control the emission in combustion engines, detection of NO_x even in low ppm range is highly demanding. A NO_x sensor is usually located at the exhaust of vehicles and includes three main components: a NO_x sensor, connecting cable, and a NO_x sensor controlling module. One of the most common methods to effectively detect NO_x in automotive systems is monitoring conductivity. For example, Pugh et al. has used ZnO inks as the metal oxide element in [147] and covered it with zeolite Y, mordenite and zeolite beta polymorph A for NO_x

detection in automotive applications. A semiconducting WO_3 covered with four types of zeolite was utilized by Zheng et al. in [148] for NO_2 detection. β - Alumina gas sensor has been developed for automotive application by Pijolat et al in [149]. Their proposed sensor includes two different solid electrolytes to detect various gases such as CO, NO, and NO_x . The experimental results confirm that the fabricated sensor is an appropriate choice for the detection of CO and NO_x . Pohle et al. has applied pulsed polarization technique on a YSZ-based sensor to detect NO_x in exhaust systems [150]. Guardiola et al. developed an estimation technique in [151] for real-time NO_x emission monitoring by using both high-frequency and low-frequency components of cylinder pressure to estimate the trapped mass, and assessing the NO_x emission cycle by cycle. Very recently, Su et al. [152] have shown that triboelectric nanogenerators have the potential to be used as a self-powered device for NO_2 detection. Although their proposed approach can be implemented at room temperature, it can be modified for specific applications in vehicle exhaust systems.

3.5.3. CO and CO_2 emission sensors

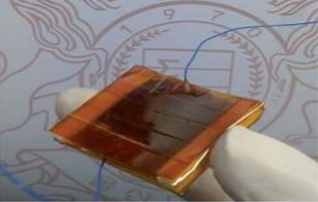
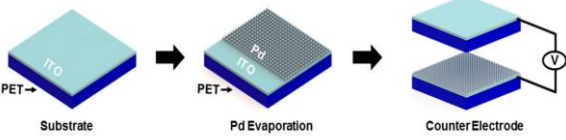
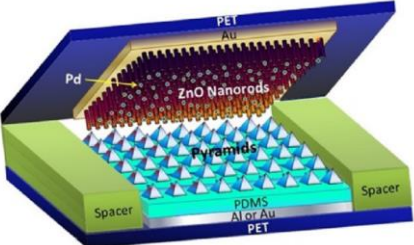
Indeed, CO is considered a “silent killer”, and is a threat to both human health and the environment. CO emissions could result in severe health problems and even death. CO concentrations higher than 400 ppm are considered poisonous to humans. In addition, CO_2 is considered a major contributor to global warming. Environmental and transportation legislations have strict rules to reduce and monitor the concentration of these two gases in ground vehicles. Consequently, developing new types of CO and CO_2 sensing devices for vehicle cabins and power generation systems are gaining momentum due to its crucial impact on passenger safety and air quality. Car companies have developed many techniques to detect and reduce these pollutants. The main three commercial technologies for vehicle cabin air quality are: electrochemical sensors, infrared-optical devices, and semiconducting metal oxide sensing devices. In addition, nanogenerators have a remarkable potential for air quality assessment in vehicle cabin.

3.5.4. Hydrogen detection sensors

Hydrogen must be monitored especially in the exhaust gas of fuel-cell vehicles [153]. As the energy source of this type of vehicle is hydrogen, it is crucial to have a cost-effective and high-resolution hydrogen sensor that meets the safety regulations. Current hydrogen monitoring

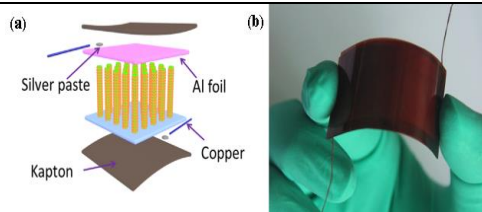
systems have Palladium-based, optical fiber-based, electrochemical-based, and MEMS-based hydrogen sensors. Nanogenerators have also shown an outstanding potential for hydrogen sensing and a few researchers have developed high-resolution hydrogen monitoring systems by using this technology [154]–[157]. Table 4 shows a few recently- developed and designed hydrogen sensors using nanogenerators, that can be implemented in automotive systems.

Table 4 Nanogenerator-based Hydrogen sensors

Sensor Mechanism and Highlights	Optical image/Schematic
<p>A self-powered TENG based hydrogen sensor using a wrinkle-micropatterned PDMS film[154]:</p> <ul style="list-style-type: none"> - An excellent low limit of detection (around 20 ppm) - High potential for energy harvesting to power itself. - Inspired portable active self-powered gas sensor. 	 <p>Image of the as-fabricated TENG-HS device; reprinted with permission [154]; Copyright Royal Society of Chemistry 2016.</p>
<p>TENG based hydrogen sensor with Pd functionalized surface [155]:</p> <ul style="list-style-type: none"> - Self-powered hydrogen sensor - Highly sensitive to hydrogen exposure - Easy to fabricate 	 <p>Schematic of the hydrogen sensor fabrication; reprinted with permission [155], Copyright MDPI 2016.</p>
<p>A TENG based hydrogen gas sensor with fast response[156]:</p> <ul style="list-style-type: none"> - Response time is about 100 s - H_2 detection resolution is about 10 ppm - Self-powered capability 	 <p>Schematic of the triboelectric-based hydrogen sensor, reprinted with permission [156]; Copyright Elsevier 2016.</p>

Portable PENG based self-Powered hydrogen sensor[157]:

- Portable hydrogen sensing package
- The detection limit is about 10 ppm
- Self-Powered capability



(a) Schematic of PENG based self-Powered hydrogen sensor, (b) optical image of the fabricated device; reprinted with permission [157]; Copyright Elsevier 2014.

4. Energy Regeneration

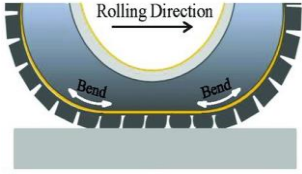


4.1. Intelligent Tires

Tires are the most essential components in vehicle stability control systems that enhance the safety of passengers and transportation systems. Thus, it is vital in the vehicle active safety systems to measure (or estimate) tire forces and aligning moments, road friction coefficient, and tire pressure. Currently, tire companies use tire pressure monitoring systems (TPMS) which can only provide information about tire pressure. In Section 3.2.1, a comprehensive review was provided on TPMS. TPMS has a lifetime limitation due to its dependence on battery life. In addition, there is no self-powered multifunctional sensor that is capable of providing information pertinent to tire forces and road conditions. In order to develop intelligent tires, which are vital for monitoring tire-road interaction, it is essential to have a combination of robust estimation techniques and durable measurement devices.

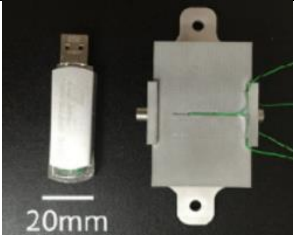
Tire-road forces have played a vital role in the field of vehicle stability control. Tire forces can be measured [158] at each corner with sensors mounted on the wheel hub, but the significant cost of available wheel transducers, required space, and calibration and maintenance make them unfeasible for mass production vehicles. Therefore, estimation of the longitudinal, lateral, and vertical tire forces using measurements available on current production vehicles, yet robust to different road conditions has been the main focus of related literature in recent years, and the topic of this section. A high gain observer with input–output linearization is proposed in [159] to estimate the lateral states. A cascaded-type tire force and vehicle sideslip angle estimator is proposed in [160] by using a sliding mode observer and Kalman filter. Steering torque measurement is used in [161], [162] for tire force estimation to address road surface friction

changes. Tire forces are estimated in [163], [164] by using a random walk model for longitudinal and lateral force evolution, an unscented Kalman filter (UKF), and planar kinetics. Recursive least square and known driving wheel torque with direct application to electric vehicles are used in [165] to estimate tire forces. In [166], a tire force estimator robust to road surface friction is developed using UKF and standard production vehicles' sensors. Corner-based longitudinal, lateral, and vertical force estimation methodologies are provided in [167]–[169] using a nonlinear observer on the wheel dynamics, an adaptive UKF on vehicle kinetics, and linear observer on the roll and pitch dynamics of the vehicle sprung mass. A modular nonlinear observer for estimation of vehicle velocities and longitudinal tire forces is proposed and tested in [170]. A tire force estimator is introduced in [171] by using wheel torque data and the Youla controller. Several approaches have been investigated for tire condition monitoring system (TCMS) such as electromagnetism, piezoelectricity, electrostatic, and nanogenerators. Among these approaches, nanogenerators have exhibited a promising potential for tire force (and moment) and road friction coefficient monitoring due to their high signal/noise ratios, low cost, flexibility, durability, sensing capabilities in harsh environments, and more importantly energy harvesting. Table 5 represents a few of recently-developed nanogenerator-based techniques for both energy harvesting and sensing in tires.

Table 4 Nanogenerators in Tires

Sensor Mechanism and Concept	Optical Images/Schematics
<p>A piezoelectric nanogenerators in tires[172]:</p> <ul style="list-style-type: none"> - Speed detection - Pressure sensing - High potential for self-powered sensing 	<div style="display: flex; justify-content: space-around;"> <div style="text-align: center;">  <p>(a)</p> </div> <div style="text-align: center;">  <p>(b)</p> </div> </div> <p>(a) Shape change of the tire during the vehicle's movement (b) photograph showing that a NG was fixed on the inner surface of a tire using adhesive tape; reprinted with permission [172]; Copyright Wiley 2011.</p>
<p>Single electrode triboelectric nanogenerators for energy harvesting from tires[173]:</p> <ul style="list-style-type: none"> - Output voltage of 55 V, and output power of 30 μW at rotation rate of $800 \frac{r}{min}$ 	<div style="text-align: center;">  </div> <p>S-TENG sensor test setup on a bicycle tire; reprinted with permission [173]; Copyright American Chemical</p>

<p>PDMS Single electrode TENG for energy harvesting from rolling tires[174]:</p> <ul style="list-style-type: none"> - Simple and scalable design. - Instantaneous power is 1.79 mW 	<p>Society 2013.</p>  <p>Schematic charge generation mechanism of the S-TENG on a rolling wheel in contact with the ground; reprinted with permission [174]; Copyright Elsevier 2015.</p>
<p>Fully-packaged and robust hybridized generator for harvesting vertical rotation energy in rolling tires[175]:</p> <ul style="list-style-type: none"> - Effectively work in a broadband of frequency - Generate a maximum energy of $10.4 \mu J$ at frequency 1 Hz. 	 <p>Schematic of a cylinder-like fully-packaged hybrid nanogenerator for harvesting vertical rotation energy; reprinted with permission [175]; Copyright Elsevier 2018.</p>
<p>A new type of TENG based device for energy harvesting from rolling tires [176]</p> <ul style="list-style-type: none"> - 500 units of CH-TENG can generate at least 1.2 W for a standard tire. - Stable and durable characteristics for a 30-day continuous experiments 	 <p>Schematic of hexagonal-structured triboelectric nanogenerators for harvesting tire rotation energy; reprinted with permission [176]; Copyright Elsevier 2018.</p>
<p>A highly flexible single electrode TENG for tire condition monitoring[28]</p> <ul style="list-style-type: none"> - Highly flexible and thermally durable TENG sensor - Potential for sensing of tire normal force 	 <p>(a) Schematic of the sidewall and attached sensor (b) top view of the sidewall of the tire with as-fabricated sensor; reprinted with permission [28]; Copyright Wiley 2017.</p>
<p>A multifunctional hybrid TENG-EMG sensor with potential application in tire condition monitoring[24]</p> <ul style="list-style-type: none"> - Highly flexible and mechanically durable - Promising to be used as a self- 	 <p>(a) Photograph of the sensor with a 1 cm scale bar (b) Photograph of the sensor attached to a tire sidewall</p>

powered sensor	(a) The fabricated self-powered sensor (b) Sidewall of attire equipped with the proposed device; reprinted with permission [24]; Copyright Elsevier 2018.
<p>A hybridized triboelectric nanogenerator for tire pressure monitoring</p> <ul style="list-style-type: none"> - Powerful enough to power a commercial wireless sensor. - Can deliver a maximal output power of 22.3 mW at the rotation speed of 100 rpm. - Durable and capable of power generating at high temperature 	 <p>The fabricated self-powered sensor for tire pressure monitoring, reprinted with permission[177];Copyright Elsevier 2018.</p>

The potential of nanogenerators for tire condition monitoring has been recently studied by Askari et al. [178] in which they predicted the future of intelligent tires and the high impact of nanogenerators to TCMS. Figure 10 shows their prediction for the future of intelligent tires.

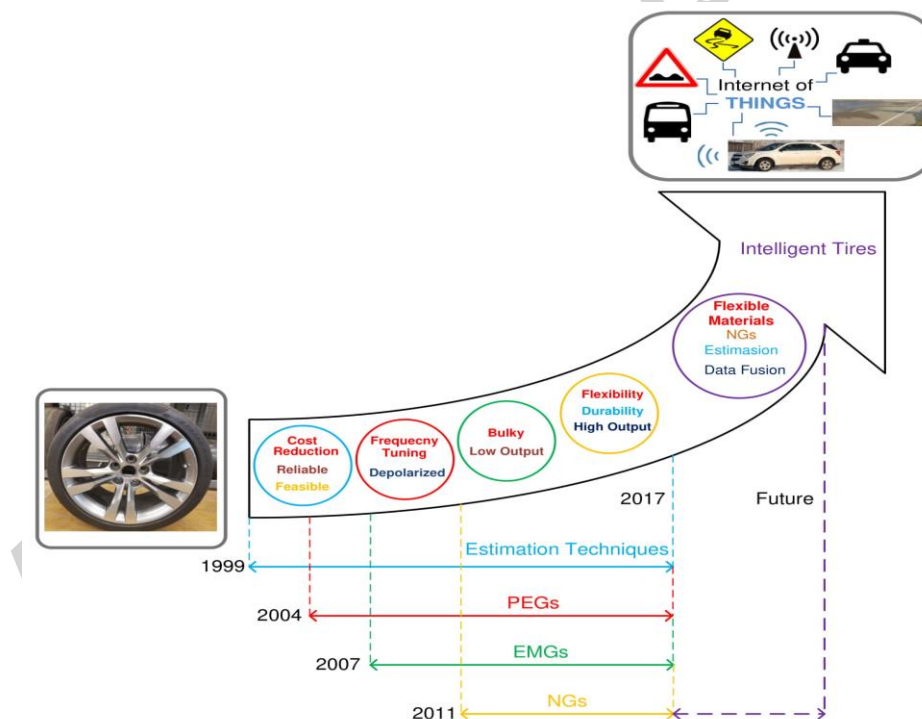
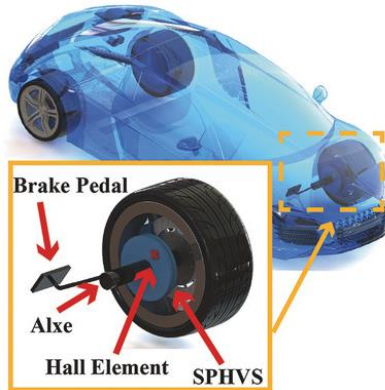


Figure 10 Evolution of intelligent tire and the prediction for future TCMS technology, reprinted with permission[178]; Copyright Wiley 2018.

Triboelectric nanogenerators can be also used for powering Hall sensor which are used for wheel speed sensing and brake monitoring. Very recently, Guo et al.[179] developed a self-powered hall sensor using triboelectric nanogenerators for wheel speed sensing and brake monitoring.

The proposed sensor demonstrates a very high rate of sensitivity for both wheel speed sensing and brake monitoring. Figure 11 schematically represents the self-powered Hall sensor[179].

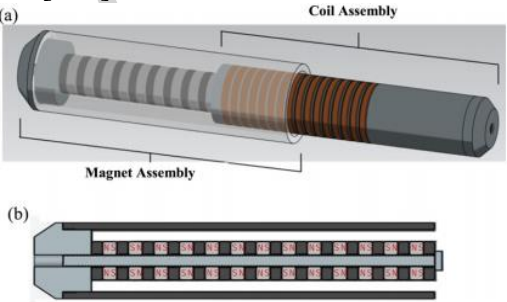
Figure 11 Schematic representation of the developed self-powered Hall sensor, reprinted with permission[179]; Copyright Wiley 2018.



4.2. Suspension

A few researchers have focused on this component of vehicles to both increase the vibration damping of the vehicle suspension, and also redesign it for energy harvesting. Thus, a number of novel designs have been proposed based on the electromagnetic concept to recover the vibration energy at high efficiency without reducing the ride comfort[180]. In table 5, a few of developed suspension systems in which electromagnetic mechanism has been used for power regeneration are presented.

Table 5 A few of developed regenerative shock absorber

Suspension system	Capability
<p data-bbox="186 1423 719 1486">An electromagnetic regenerative shock absorber[180]</p>  <p data-bbox="186 1801 885 1873">(a) Diagram of the linear electromagnetic shock absorber and (b) the cross section of the magnet</p>	<ul style="list-style-type: none"> <li data-bbox="938 1600 1433 1711">- It can harvest 16-64 Watt at 0.25-0.5 ms^{-1} RMS suspension velocity.

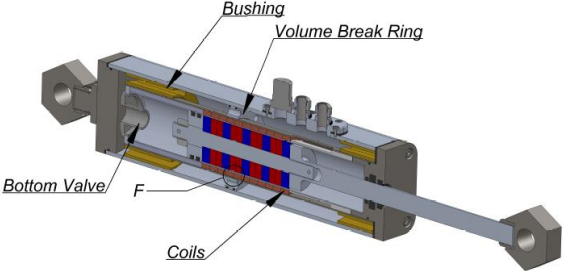

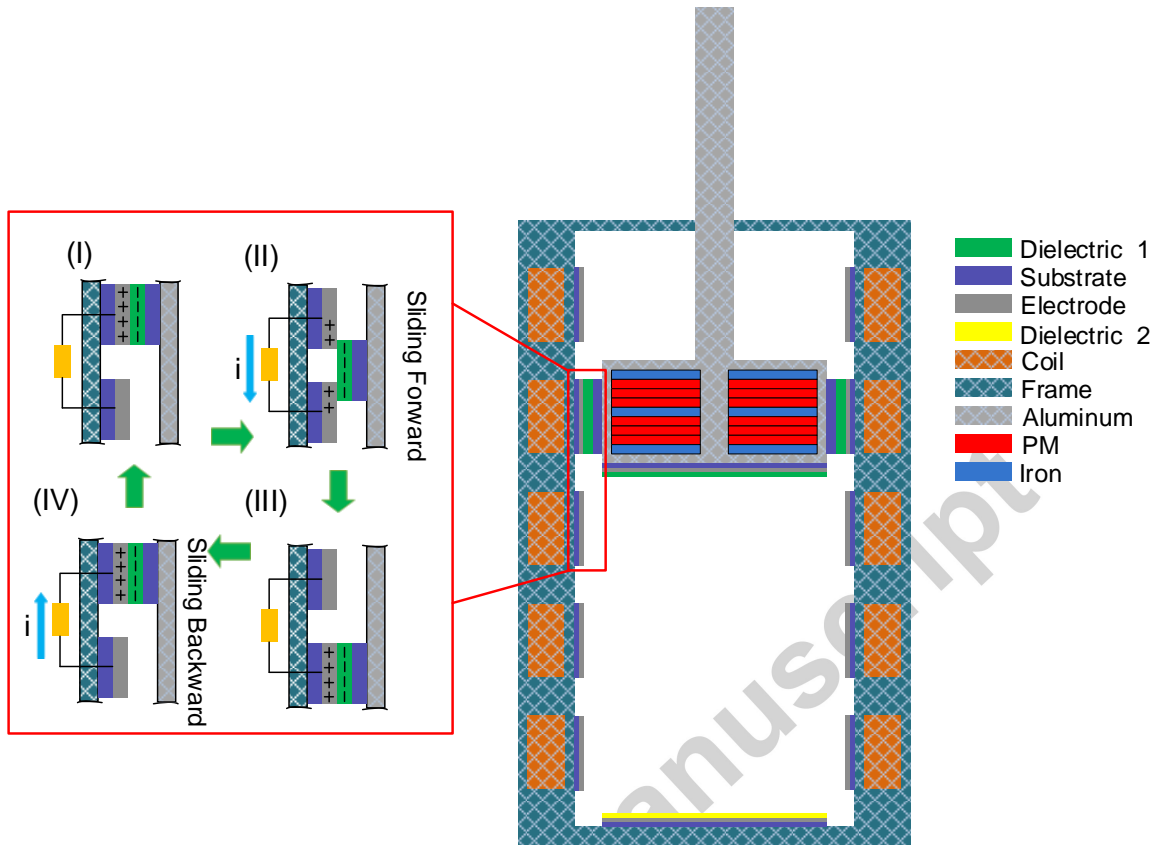
<p>assembly; reprinted with permission [180]; Copyright IOP Science 2010.</p>	
<p>Regenerative and Adaptive Shock absorber [181], [182],</p>  <p>Hybrid damper twin tube design , reprinted with permission [183].</p>	<ul style="list-style-type: none"> - Capable of providing variable damping coefficient in the range of 1302–1540 $N.s/m$. - It can generate approximately 80 Watt at excitation amplitude of 14 mm and frequency of 15 Hz.
<p>Electromagnetic-pneumatic hybrid actuator[183]:</p>  <p>Fabricated electromagnetic-pneumatic hybrid actuator; reprinted with permission [183].</p>	<ul style="list-style-type: none"> - Hydraulic damping of 1300 $N.s/m$ - Electromagnetic variable damping of 0-240 $N.s/m$.

Figure 12 shows a conceptual design for a regenerative shock absorber with a combination of electromagnetism and triboelectric nanogenerators. The combination of the developed electromagnetic regenerative absorber in Ref. [181], [182] and grating TENGs, as presented in Figure 12, increases the energy regeneration capability of the shock absorber. The presented conceptual design in Figure 12 combines two different modes of TENGs including sliding and contact-separation modes. Developing an optimized configuration for both electromagnetic and TENG components of the proposed conceptual device enhances the energy conversion efficiency of the shock absorber.

Figure 12 Conceptual design of hybridized electromagnetic-triboelectric regenerative shock absorber.



5. Conclusion, perspectives and challenges

In this review article, different types of sensing mechanisms in vehicle systems were reviewed. Some of the main techniques for sensing and energy harvesting, such as electromagnetic generators, Hall effect, eddy current, and AMR were first described. Afterwards, we illustrated the new techniques of sensing and energy harvesting by implementing nanogenerators. The second section of this review article covered five different categories of sensing in automotive systems including position sensors, thermal sensors, chemical and gas sensors, inertial measurement unit, and pressure sensors. For each of these sensing categories, it was shown that NGs could be implemented to improve the current automotive sensory technologies. Nanogenerators could also be used for developing a number of novel sensors for vehicle systems. In Table 6, we provide a short list of the sensors and devices which can be improved to self-powered category in automotive and vehicle active safety systems using nanogenerators.

Table 6 List of the potential self-powered sensors using nanogenerators for automotive systems

Device Category	Potential Application in Vehicles	Technology/operating mode
Position Sensors	Steering wheel position self-powered sensor	TENG/ Sliding mode
	Pedal position self-powered sensor	TENG/ Contact-Separation
	Fuel level self-powered sensor	TENG/ Sliding mode
	Wheel speed self-powered sensor	TENG/ Sliding mode
	Throttle position self-powered sensor	TENG/Sliding mode
	Chassis height self-powered sensor	TENG/Sliding mode
Thermal Sensors	Engine coolant self-powered temperature sensor	PYNG
	Exhaust gas self-powered temperature sensor	PYNG
Gas and Chemical Composition Sensors	CO and CO ₂ self-powered sensor	TENG-PENG
	NO _x detection self-powered sensor	TENG-PENG
	H ₂ detection self-powered sensor	TENG-PENG
	Humidity detection self-powered sensor	TENG-PENG
Pressure sensor	Self-powered TPMS	TENG-PENG
Other NGs based sensors and devices	Driver's cabin self-powered touch pad	TENG-PENG
	Self-powered occupant sensor	TENG/ Contact-Separation
	Self-powered seat belt sensor	TENG/ Contact-Separation
Intelligent Tires	Self-powered sensor for TCMS	TENG-PENG

Nanogenerators can be used not only for self-powered sensing but also, for energy harvesting, as we presented a conceptual design for hybridized electromagnetic-triboelectric regenerative shock absorber. For developing new types of sensors for vehicle systems we need to draw on different disciplines including nanogenerators, vehicle dynamics, material science and sensing systems to accelerate the development of future rolling computers. There are a few main challenges in developing self-powered sensors based on nanogenerators for vehicle systems that should be addressed by researchers. The first challenge is related to the selection of an appropriate set of materials for fabrication of sensors with high thermal and mechanical durability for specific applications in automotive systems. For example, tires have a very harsh environment and developing a durable and reliable self-powered sensor for them is a very challenging task. Another potential challenge can be related to processing of the obtained data through the novel self-powered sensors using nanogenerators. In order to address this challenge, expertise from other disciplines such as computer sciences, neural and sensor networks is inescapable. The last challenge is related to the capability of creating line of production to fabricate the final set of self-powered devices for automotive applications.

References

- [1] J. C. Maxwell, "VIII. A dynamical theory of the electromagnetic field," *Philos. Trans. R. Soc. London*, vol. 155, pp. 459–512, 1865.
- [2] Z. L. Wang, "On Maxwell's displacement current for energy and sensors: the origin of nanogenerators," *Mater. Today*, vol. 20, no. 2, pp. 74–82, Mar. 2017.
- [3] M. J. Caruso and L. S. Withanawasam, "Vehicle detection and compass applications using AMR magnetic sensors," in *Sensors Expo Proceedings*, 1999, vol. 477, p. 39.
- [4] C. P. O. Treutler, "Magnetic sensors for automotive applications," *Sensors Actuators A Phys.*, vol. 91, no. 1, pp. 2–6, 2001.
- [5] D. L. Striker and R. J. Hampo, "Method of position sensing utilizing giant magneto resistance elements and solid state switch array." Google Patents, 27-Jul-1999.
- [6] D. Nachtigal and G. Bergmann, "Multi-Pole Magnetic Encoders for Active Speed-Measurement Systems." SAE International, 1999.
- [7] T. Wang, Z. Jiao, and L. Yan, "Design and Comparative Study of Dual Magnet Array for Linear Load Simulation System," in *Vehicle Power and Propulsion Conference (VPPC), 2016 IEEE*, 2016, pp. 1–5.
- [8] C. R. Bowen and M. H. Arafa, "Energy Harvesting Technologies for Tire Pressure Monitoring Systems," *Adv. Energy Mater.*, vol. 5, no. 7, p. n/a–n/a, Apr. 2015.
- [9] K. Mohri, "Review on recent advances in the field of amorphous-metal sensors and transducers," *IEEE Trans. Magn.*, vol. 20, no. 5, pp. 942–947, 1984.
- [10] G. R. Kohut, J. Y. Yoon, M. D. Murphy, D. L. Hartley, and D. B. Purdie, "Seat belt tension sensor." Google Patents, 29-Apr-2003.
- [11] H. S. Husby, V. C. Patel, and A. F. Patel, "Seat belt buckle sensor." Google Patents, 05-Oct-1999.
- [12] T. M. Frusti and M. N. Williams, "Occupant restraint system with seat position sensor." Google Patents, 25-Apr-2000.
- [13] W. Thomson, "XIX. On the electro-dynamic qualities of metals:—Effects of magnetization on the electric conductivity of nickel and of iron," *Proc. R. Soc. London*, vol. 8, pp. 546–550, 1857.
- [14] L. Jogschies, D. Klaas, R. Kruppe, J. Rittinger, P. Taptimthong, A. Wienecke, L. Rissing, and M. C. Wurcz, "Recent developments of magnetoresistive sensors for industrial applications," *Sensors*, vol. 15, no. 11, pp. 28665–28689, 2015.
- [15] E. H. Hall, "On a new action of the magnet on electric currents," *Am. J. Math.*, vol. 2, no. 3, pp. 287–292, 1879.
- [16] F. Townsend, "Eddy current losses in transformers," *Trans. Am. Inst. Electr. Eng.*, vol. 17, pp. 319–334, 1900.
- [17] Z. L. Wang, "Triboelectric nanogenerators as new energy technology for self-powered

- systems and as active mechanical and chemical sensors,” *ACS Nano*, vol. 7, no. 11, pp. 9533–9557, 2013.
- [18] Z. L. Wang, J. Chen, and L. Lin, “Progress in triboelectric nanogenerators as a new energy technology and self-powered sensors,” *Energy Environ. Sci.*, vol. 8, no. 8, pp. 2250–2282, 2015.
- [19] F. R. Fan, W. Tang, and Z. L. Wang, “Flexible Nanogenerators for Energy Harvesting and Self-Powered Electronics,” *Adv. Mater.*, Jan. 2016.
- [20] H. Guo, Z. Wen, Y. Zi, M.-H. Yeh, J. Wang, L. Zhu, C. Hu, and Z. L. Wang, “A Water-Proof Triboelectric–Electromagnetic Hybrid Generator for Energy Harvesting in Harsh Environments,” *Adv. Energy Mater.*, vol. 6, no. 6, p. 1501593–n/a, Mar. 2016.
- [21] Y. Hu, J. Yang, Q. Jing, S. Niu, W. Wu, and Z. L. Wang, “Triboelectric Nanogenerator Built on Suspended 3D Spiral Structure as Vibration and Positioning Sensor and Wave Energy Harvester,” *ACS Nano*, vol. 7, no. 11, pp. 10424–10432, Nov. 2013.
- [22] S. Niu and Z. L. Wang, “Theoretical systems of triboelectric nanogenerators,” *Nano Energy*, vol. 14, pp. 161–192, May 2015.
- [23] H. Askari, E. Asadi, Z. Saadatnia, A. Khajepour, M. B. Khamesee, and J. Zu, “A hybridized electromagnetic-triboelectric self-powered sensor for traffic monitoring: concept, modelling, and optimization,” *Nano Energy*, vol. 32, no. Supplement C, pp. 105–116, 2017.
- [24] H. Askari, Z. Saadatnia, E. Asadi, A. Khajepour, M. B. Khamesee, and J. Zu, “A flexible hybridized electromagnetic-triboelectric multi-purpose self-powered sensor,” *Nano Energy*, vol. 45, pp. 319–329, 2018.
- [25] Z. Saadatnia, E. Asadi, H. Askari, J. Zu, and E. Esmailzadeh, “Modeling and performance analysis of duck-shaped triboelectric and electromagnetic generators for water wave energy harvesting,” *Int. J. Energy Res.*, 2017.
- [26] Z. Saadatnia, E. Asadi, H. Askari, E. Esmailzadeh, and H. E. Naguib, “A heaving point absorber-based triboelectric-electromagnetic wave energy harvester: An efficient approach toward blue energy,” *Int. J. Energy Res.*, 2018.
- [27] Y. Bian, T. Jiang, T. Xiao, W. Gong, X. Cao, Z. Wang, and Z. L. Wang, “Triboelectric Nanogenerator Tree for Harvesting Wind Energy and Illuminating in Subway Tunnel,” *Adv. Mater. Technol.*, 2018.
- [28] H. Askari, Z. Saadatnia, A. Khajepour, M. B. Khamesee, and J. Zu, “A Triboelectric Self-Powered Sensor for Tire Condition Monitoring: Concept, Design, Fabrication, and Experiments,” *Adv. Eng. Mater.*
- [29] P. Maharjan, R. M. Toyabur, and J. Y. Park, “A human locomotion inspired hybrid nanogenerator for wrist-wearable electronic device and sensor applications,” *Nano Energy*, vol. 46, pp. 383–395, 2018.
- [30] M. Salauddin, R. M. Toyabur, P. Maharjan, and J. Y. Park, “High performance human-induced vibration driven hybrid energy harvester for powering portable electronics,” *Nano*

- Energy*, vol. 45, pp. 236–246, 2018.
- [31] S. Wang, L. Lin, and Z. L. Wang, “Triboelectric nanogenerators as self-powered active sensors,” *Nano Energy*, vol. 11, pp. 436–462, 2015.
- [32] Z. L. Wang, L. Lin, J. Chen, S. Niu, and Y. Zi, *Triboelectric Nanogenerators*. Springer International Publishing, 2016.
- [33] S. Wang, L. Lin, Y. Xie, Q. Jing, S. Niu, and Z. L. Wang, “Sliding-Triboelectric Nanogenerators Based on In-Plane Charge-Separation Mechanism,” *Nano Lett.*, vol. 13, no. 5, pp. 2226–2233, May 2013.
- [34] M. Wang, N. Zhang, Y. Tang, H. Zhang, C. Ning, L. Tian, W. Li, J. Zhang, Y. Mao, and E. Liang, “Single-electrode triboelectric nanogenerators based on sponge-like porous PTFE thin films for mechanical energy harvesting and self-powered electronics,” *J. Mater. Chem. A*, vol. 5, no. 24, pp. 12252–12257, 2017.
- [35] Z. L. Wang and J. Song, “Piezoelectric nanogenerators based on zinc oxide nanowire arrays,” *Science*, vol. 312, no. 5771, pp. 242–6, Apr. 2006.
- [36] X. Wang, “Piezoelectric nanogenerators—Harvesting ambient mechanical energy at the nanometer scale,” *Nano Energy*, vol. 1, no. 1, pp. 13–24, Jan. 2012.
- [37] Y. Gao and Z. L. Wang, “Electrostatic potential in a bent piezoelectric nanowire. The fundamental theory of nanogenerator and nanopiezotronics,” *Nano Lett.*, vol. 7, no. 8, pp. 2499–2505, 2007.
- [38] G. Zhu, A. C. Wang, Y. Liu, Y. Zhou, and Z. L. Wang, “Functional electrical stimulation by nanogenerator with 58 V output voltage,” *Nano Lett.*, vol. 12, no. 6, pp. 3086–3090, 2012.
- [39] B. Kumar and S.-W. Kim, “Energy harvesting based on semiconducting piezoelectric ZnO nanostructures,” *Nano Energy*, vol. 1, no. 3, pp. 342–355, 2012.
- [40] Z. Wen, Q. Shen, and X. Sun, “Nanogenerators for Self-Powered Gas Sensing,” *Nano-Micro Lett.*, vol. 9, no. 4, p. 45, 2017.
- [41] X. Wang, J. Song, J. Liu, and Z. L. Wang, “Direct-current nanogenerator driven by ultrasonic waves,” *Science (80-.)*, vol. 316, no. 5821, pp. 102–105, 2007.
- [42] M.-Y. Choi, D. Choi, M.-J. Jin, I. Kim, S.-H. Kim, J.-Y. Choi, S. Y. Lee, J. M. Kim, and S.-W. Kim, “Mechanically powered transparent flexible charge-generating nanodevices with piezoelectric ZnO nanorods,” *Adv. Mater.*, vol. 21, no. 21, pp. 2185–2189, 2009.
- [43] B. Kumar and S.-W. Kim, “Recent advances in power generation through piezoelectric nanogenerators,” *J. Mater. Chem.*, vol. 21, no. 47, pp. 18946–18958, 2011.
- [44] S. N. Cha, J.-S. Seo, S. M. Kim, H. J. Kim, Y. J. Park, S.-W. Kim, and J. M. Kim, “Sound-driven piezoelectric nanowire-based nanogenerators,” *Adv. Mater.*, vol. 22, no. 42, pp. 4726–4730, 2010.
- [45] X. Chen, S. Xu, N. Yao, and Y. Shi, “1.6 v nanogenerator for mechanical energy harvesting using PZT nanofibers,” *Nano Lett.*, vol. 10, no. 6, pp. 2133–2137, 2010.

- [46] Y. Qin, X. Wang, and Z. L. Wang, "Microfibre–nanowire hybrid structure for energy scavenging," *Nature*, vol. 451, p. 809, Feb. 2008.
- [47] Y. Hu, Y. Zhang, C. Xu, G. Zhu, and Z. L. Wang, "High-Output Nanogenerator by Rational Unipolar Assembly of Conical Nanowires and Its Application for Driving a Small Liquid Crystal Display," *Nano Lett.*, vol. 10, no. 12, pp. 5025–5031, Dec. 2010.
- [48] K. Liu, T. Ding, J. Li, Q. Chen, G. Xue, P. Yang, M. Xu, Z. L. Wang, and J. Zhou, "Thermal–Electric Nanogenerator Based on the Electrokinetic Effect in Porous Carbon Film," *Adv. Energy Mater.*, vol. 8, no. 13, p. 1702481, 2018.
- [49] K. Liu, Y. Zhou, F. Yuan, X. Mo, P. Yang, Q. Chen, J. Li, T. Ding, and J. Zhou, "Self-Powered Multimodal Temperature and Force Sensor Based-On a Liquid Droplet," *Angew. Chemie Int. Ed.*, vol. 55, no. 51, pp. 15864–15868, 2016.
- [50] P. Yang, K. Liu, Q. Chen, X. Mo, Y. Zhou, S. Li, G. Feng, and J. Zhou, "Wearable thermocells based on gel electrolytes for the utilization of body heat," *Angew. Chemie Int. Ed.*, vol. 55, no. 39, pp. 12050–12053, 2016.
- [51] Y. Yang, W. Guo, K. C. Pradel, G. Zhu, Y. Zhou, Y. Zhang, Y. Hu, L. Lin, and Z. L. Wang, "Pyroelectric nanogenerators for harvesting thermoelectric energy," *Nano Lett.*, vol. 12, no. 6, pp. 2833–2838, 2012.
- [52] Y. Yang, S. Wang, Y. Zhang, and Z. L. Wang, "Pyroelectric nanogenerators for driving wireless sensors," *Nano Lett.*, vol. 12, no. 12, pp. 6408–6413, 2012.
- [53] Y. Yang, Y. Zhou, J. M. Wu, and Z. L. Wang, "Single Micro/Nanowire Pyroelectric Nanogenerators as Self-Powered Temperature Sensors," *ACS Nano*, vol. 6, no. 9, pp. 8456–8461, Sep. 2012.
- [54] S. C. Bera, H. Mandal, S. Saha, and A. Dutta, "Study of a modified capacitance-type level transducer for any type of liquid," *IEEE Trans. Instrum. Meas.*, vol. 63, no. 3, pp. 641–649, 2014.
- [55] B. Kumar, G. Rajita, and N. Mandal, "A review on capacitive-type sensor for measurement of height of liquid level," *Meas. Control*, vol. 47, no. 7, pp. 219–224, 2014.
- [56] K. A. P. Menon and R. Hariharan, "A new liquid level sensor for process-control applications," *IEEE Trans. Instrum. Meas.*, vol. 28, no. 2, pp. 155–158, 1979.
- [57] S. C. Bera, J. K. Ray, and S. Chattopadhyay, "A low-cost noncontact capacitance-type level transducer for a conducting liquid," *IEEE Trans. Instrum. Meas.*, vol. 55, no. 3, pp. 778–786, 2006.
- [58] Y.-T. Li, C.-M. Chao, and K. Wang, "A capacitance level sensor design and sensor signal enhancement," in *Nano/Micro Engineered and Molecular Systems (NEMS), 2011 IEEE International Conference on*, 2011, pp. 847–850.
- [59] G. Betta, A. Pietrosanto, and A. Scaglione, "A gray-code-based fiber optic liquid level transducer," *IEEE Trans. Instrum. Meas.*, vol. 47, no. 1, pp. 174–178, 1998.
- [60] B. Yun, N. Chen, and Y. Cui, "Highly sensitive liquid-level sensor based on etched fiber

- Bragg grating,” *IEEE photonics Technol. Lett.*, vol. 19, no. 21, pp. 1747–1749, 2007.
- [61] D. Royer, L. Levin, and O. Legras, “A liquid level sensor using the absorption of guided acoustic waves,” *IEEE Trans. Ultrason. Ferroelectr. Freq. Control*, vol. 40, no. 4, pp. 418–421, 1993.
- [62] D. Choi, S. Lee, S. M. Park, H. Cho, W. Hwang, and D. S. Kim, “Energy harvesting model of moving water inside a tubular system and its application of a stick-type compact triboelectric nanogenerator,” *Nano Res.*, vol. 8, no. 8, p. 2481, 2015.
- [63] G. Zhu, Y. Su, P. Bai, J. Chen, Q. Jing, W. Yang, and Z. L. Wang, “Harvesting water wave energy by asymmetric screening of electrostatic charges on a nanostructured hydrophobic thin-film surface,” *ACS Nano*, vol. 8, no. 6, pp. 6031–6037, 2014.
- [64] W. J. Fleming, “Overview of Automotive Sensors,” *IEEE Sens. J.*, vol. 1, no. 4, pp. 296–308, 2001.
- [65] A. M. Madni and R. F. Wells, “Advanced steering wheel sensor,” *Sensors (Peterborough, NH)*, vol. 17, no. 2, pp. 28,30,32–35,38,40, 2000.
- [66] D. J. Adelerhof and W. Geven, “New position detectors based on AMR sensors,” *Sensors Actuators A Phys.*, vol. 85, no. 1, pp. 48–53, 2000.
- [67] R. White, “Tire pressure monitoring system mandate drives technology,” *Automot. Ind. AI*, vol. 187, no. 9, 2007.
- [68] K. T. Sterne, J. M. Ernst, D. K. Kilcoyne, A. J. Michaels, and G. Moy, “Tire pressure monitoring system sensor radio frequency measurements for privacy concerns,” *Transportation Research Record*, vol. 2643, pp. 34–44, 2017.
- [69] D. K. Kilcoyne, S. Bendelac, J. M. Ernst, and A. J. Michaels, “Tire Pressure Monitoring System encryption to improve vehicular security,” 2016, pp. 1219–1224.
- [70] G. Lasser and C. F. Mecklenbräuker, “Channel model for Tyre pressure monitoring systems (TPMS),” 2010.
- [71] G. J. Nga, “Study on Electromagnetic Wave Propagation Characteristics in Rotating Environments and Its Application in Tire Pressure Monitoring,” *IEEE Trans. Instrum. Meas.*, vol. 61, no. 6, pp. 1765–1777, Jun. 2012.
- [72] H. J. Song, H. P. Hsu, R. Wiese, and T. Talty, “Modeling signal strength range of TPMS in automobiles,” 2004, vol. 3, pp. 3167–3170.
- [73] G. Lasser and C. F. Mecklenbräuker, “Dual-band channel measurements for an advanced tyre monitoring system,” 2010.
- [74] M. Pavlin and F. Novak, “Yield enhancement of piezoresistive pressure sensors for automotive applications,” *Sensors Actuators A Phys.*, vol. 141, no. 1, pp. 34–42, 2008.
- [75] B.-N. Lee, K.-N. Kim, H.-D. Park, and S.-M. Shin, “Calibration and temperature compensation of silicon pressure sensors using ion-implanted trimming resistors,” *Sensors Actuators A Phys.*, vol. 72, no. 2, pp. 148–152, 1999.

- [76] Y. Hata, K. Ikeura, T. Morita, and T. Abo, "Engine control system using a cylinder pressure sensor," *IEE Proc. D - Control Theory Appl.*, vol. 136, no. 2, pp. 84–88, 1989.
- [77] J. D. Powell, "Engine Control Using Cylinder Pressure: Past, Present, and Future," *J. Dyn. Syst. Meas. Control*, vol. 115, no. 2B, pp. 343–350, Jun. 1993.
- [78] M. T. Wlodarczyk, "High Accuracy Glow Plug-Integrated Cylinder Pressure Sensor for Closed Loop Engine Control." SAE International, 2006.
- [79] F. Tagliatalata-Scafati, M. Lavorgna, E. Mancaruso, and B. M. Vaglieco, *Nonlinear Systems and Circuits in Internal Combustion Engines: Modeling and Control*. Springer International Publishing, 2017.
- [80] K. Sawamoto, Y. Kawamura, T. Kita, and K. Matsushita, "Individual Cylinder Knock Control by Detecting Cylinder Pressure." SAE International, 1987.
- [81] E. H. Gassenfeit and J. D. Powell, "Algorithms for air-fuel ratio estimation using internal combustion engine cylinder pressure," 1989.
- [82] J. C. Gilkey and J. D. Powell, "Fuel-air ratio determination from cylinder pressure time histories," *J. Dyn. Syst. Meas. Control. Trans. ASME*, vol. 107, no. 4, pp. 252–257, 1985.
- [83] P. K. Houpt and S. K. Andreadakis, "Estimation of fuel-air ratio from cylinder pressure in spark ignited engines," 1983.
- [84] R. S. Patrick and J. D. Powell, "A technique for the real-time estimation of air-fuel ratio using molecular weight ratios," 1990.
- [85] A. Yazdani, J. Naber, M. Shahbakhti, P. Dice, C. Glugla, S. Cooper, D. McEwan, and G. Huberts, "Air Charge and Residual Gas Fraction Estimation for a Spark-Ignition Engine Using In-Cylinder Pressure," vol. 2017-March, no. March, 2017.
- [86] R. Di Leo, "Methodologies for air-fuel ratio and trapped mass estimation in diesel engines using the in-cylinder pressure measurement," 2015, vol. 82, pp. 957–964.
- [87] S. J. Citron, J. E. O'Higgins, and L. Y. Chen, "Cylinder by cylinder engine pressure and pressure torque waveform determination utilizing speed fluctuations," 1989.
- [88] M. H. Salah, T. H. Mitchell, J. R. Wagner, and D. M. Dawson, "Nonlinear-control strategy for advanced vehicle thermal-management systems," *IEEE Trans. Veh. Technol.*, vol. 57, no. 1, pp. 127–137, 2008.
- [89] M. Abu-Qudais, "Exhaust gas temperature for knock detection and control in spark ignition engine," *Energy Convers. Manag.*, vol. 37, no. 9, pp. 1383–1392, 1996.
- [90] H. Xue, Q. Yang, D. Wang, W. Luo, W. Wang, M. Lin, D. Liang, and Q. Luo, "A wearable pyroelectric nanogenerator and self-powered breathing sensor," *Nano Energy*, vol. 38, pp. 147–154, 2017.
- [91] B. Montaron, "Automotive thick film temperature sensors," 1983.
- [92] J. E. Acker, "TEMPERATURE SENSORS FOR ELECTRONIC ENGINE CONTROL SYSTEMS.," *SAE Prepr*, no. 780211, 1978.

- [93] A. A. Kenny, C. F. Bradshaw, and B. T. Creed, "Electronic thermostat system for automotive engines," 1988.
- [94] W. Krause and K. H. Spies, "Dynamic control of the coolant temperature for a reduction of fuel consumption and hydrocarbon emission," 1996.
- [95] J. Carter, "Thermistor control of engine coolant systems," *Sensors (Peterborough, NH)*, vol. 13, no. 9 pt 1, pp. 65–68, 1996.
- [96] H. Yamaguchi, K. Sawamoto, H. Sanbuichi, T. Morita, and S. Takizawa, "Back-up system and method for engine coolant temperature sensor in electronic engine control system." Google Patents, 03-Dec-1985.
- [97] C. S. Newman, "MONITORING ENGINE COOLANT." US Patent App. 15/493,009, 23-Nov-2017.
- [98] S. M. Erlien, S. Fujita, and J. C. Gerdes, "Shared steering control using safe envelopes for obstacle avoidance and vehicle stability," *IEEE Trans. Intell. Transp. Syst.*, vol. 17, no. 2, pp. 441–451, 2016.
- [99] N. Lu, N. Cheng, N. Zhang, X. Shen, and J. W. Mark, "Connected vehicles: Solutions and challenges," *IEEE internet things J.*, vol. 1, no. 4, pp. 289–299, 2014.
- [100] M. Jalali, A. Khajepour, S. Chen, and B. Litkouhi, "Integrated stability and traction control for electric vehicles using model predictive control," *Control Eng. Pract.*, vol. 54, pp. 256–266, 2016.
- [101] J. Ryu and J. C. Gerdes, "Integrating inertial sensors with global positioning system (GPS) for vehicle dynamics control," *J. Dyn. Syst. Meas. Control*, vol. 126, no. 2, pp. 243–254, 2004.
- [102] L. Imsland, T. A. Johansen, T. I. Fossen, H. F. Grip, J. C. Kalkkuhl, and A. Suissa, "Vehicle velocity estimation using nonlinear observers," *Automatica*, vol. 42, no. 12, pp. 2091–2103, 2006.
- [103] D. Selmanaj, M. Corno, G. Panzani, and S. M. Savaresi, "Vehicle sideslip estimation: A kinematic based approach," *Control Eng. Pract.*, vol. 67, pp. 1–12, 2017.
- [104] D. M. Bevly, J. Ryu, and J. C. Gerdes, "Integrating INS sensors with GPS measurements for continuous estimation of vehicle sideslip, roll, and tire cornering stiffness," *IEEE Trans. Intell. Transp. Syst.*, vol. 7, no. 4, pp. 483–493, 2006.
- [105] J. A. Farrell, H.-S. Tan, and Y. Yang, "Carrier phase GPS-aided INS-based vehicle lateral control," *J. Dyn. Syst. Meas. Control*, vol. 125, no. 3, pp. 339–353, 2003.
- [106] J.-H. Yoon and H. Peng, "A cost-effective sideslip estimation method using velocity measurements from two GPS receivers," *IEEE Trans. Veh. Technol.*, vol. 63, no. 6, pp. 2589–2599, 2014.
- [107] J.-H. Yoon and H. Peng, "Robust vehicle sideslip angle estimation through a disturbance rejection filter that integrates a magnetometer with GPS," *IEEE Trans. Intell. Transp. Syst.*, vol. 15, no. 1, pp. 191–204, 2014.

- [108] E. Hashemi, M. Pirani, A. Khajepour, B. Fidan, A. Kasaiezadeh, and S.-K. Chen, "Opinion Dynamics-Based Vehicle Velocity Estimation and Diagnosis," *IEEE Trans. Intell. Transp. Syst.*, 2017.
- [109] X. Niu, S. Nasser, C. Goodall, and N. El-Sheimy, "A universal approach for processing any MEMS inertial sensor configuration for land-vehicle navigation," *J. Navig.*, vol. 60, no. 2, pp. 233–245, 2007.
- [110] B. Phuyal, "An experiment for a 2-D and 3-D GPS/INS configuration for land vehicle applications," in *Position Location and Navigation Symposium, 2004. PLANS 2004*, 2004, pp. 148–152.
- [111] S. P. Won, W. W. Melek, and F. Golnaraghi, "A Kalman/particle filter-based position and orientation estimation method using a position sensor/inertial measurement unit hybrid system," *IEEE Trans. Ind. Electron.*, vol. 57, no. 5, pp. 1787–1798, 2010.
- [112] A. Ramezani, A. Alasty, and J. Akbari, "Effects of rotary inertia and shear deformation on nonlinear free vibration of microbeams," vol. 128, no. 5, pp. 611–615, Oct. 2006.
- [113] U. Maeder and M. Morari, "Attitude estimation for vehicles with partial inertial measurement," *IEEE Trans. Veh. Technol.*, vol. 60, no. 4, pp. 1496–1504, 2011.
- [114] T. Chu, N. Guo, S. Backén, and D. Akos, "Monocular camera/IMU/GNSS integration for ground vehicle navigation in challenging GNSS environments," *Sensors*, vol. 12, no. 3, pp. 3162–3185, 2012.
- [115] H. Lategahn, M. Schreiber, J. Ziegler, and C. Stiller, "Urban localization with camera and inertial measurement unit," in *Intelligent Vehicles Symposium (IV), 2013 IEEE*, 2013, pp. 719–724.
- [116] T. W. Follmer and S. McClellan, "System and method for viewing and correcting data in a street mapping database." Google Patents, 24-Feb-2015.
- [117] E. Hashemi, R. Zarringhalam, A. Khajepour, W. Melek, A. Kasaiezadeh, and S.-K. Chen, "Real-time estimation of the road bank and grade angles with unknown input observers," *Veh. Syst. Dyn.*, vol. 55, no. 5, pp. 648–667, 2017.
- [118] A. Noureldin, T. B. Karamat, M. D. Eberts, and A. El-Shafie, "Performance enhancement of MEMS-based INS/GPS integration for low-cost navigation applications," *IEEE Trans. Veh. Technol.*, vol. 58, no. 3, pp. 1077–1096, 2009.
- [119] F. Höflinger, J. Müller, R. Zhang, L. M. Reindl, and W. Burgard, "A wireless micro inertial measurement unit (IMU)," *IEEE Trans. Instrum. Meas.*, vol. 62, no. 9, pp. 2583–2595, 2013.
- [120] W. Ochieng, J. W. Polak, R. Noland, J.-Y. Park, L. Zhao, D. Briggs, J. Gulliver, A. Crookell, R. Evans, and M. Walker, "Integration of GPS and dead reckoning for real-time vehicle performance and emissions monitoring," *GPS Solut.*, vol. 6, no. 4, pp. 229–241, 2003.
- [121] Y. K. Peng and M. F. Golnaraghi, "A vector-based gyro-free inertial navigation system by integrating existing accelerometer network in a passenger vehicle," in *Position Location*

- and Navigation Symposium, 2004. PLANS 2004*, 2004, pp. 234–242.
- [122] D. M. Bevly, “Global positioning system (GPS): A low-cost velocity sensor for correcting inertial sensor errors on ground vehicles,” *J. Dyn. Syst. Meas. Control*, vol. 126, no. 2, pp. 255–264, 2004.
- [123] D. Sun, M. G. Petovello, and M. E. Cannon, “GPS/reduced IMU with a local terrain predictor in land vehicle navigation,” *Int. J. Navig. Obs.*, vol. 2008, 2008.
- [124] U. Iqbal, A. F. Okou, and A. Noureldin, “An integrated reduced inertial sensor system—RISS/GPS for land vehicle,” in *Position, Location and Navigation Symposium, 2008 IEEE/ION*, 2008, pp. 1014–1021.
- [125] S. Han and J. Wang, “Land vehicle navigation with the integration of GPS and reduced INS: performance improvement with velocity aiding,” *J. Navig.*, vol. 63, no. 1, pp. 153–166, 2010.
- [126] P. Schopp, L. Klingbeil, C. Peters, and Y. Manoli, “Design, geometry evaluation, and calibration of a gyroscope-free inertial measurement unit,” *Sensors Actuators A Phys.*, vol. 162, no. 2, pp. 379–387, 2010.
- [127] D. Sun, *Ultra-tight GPS/reduced IMU for land vehicle navigation*, vol. 71, no. 08. 2010.
- [128] H. Zhang, Y. Wu, W. Wu, M. Wu, and X. Hu, “Improved multi-position calibration for inertial measurement units,” *Meas. Sci. Technol.*, vol. 21, no. 1, p. 15107, 2009.
- [129] L. Jin, S. Ma, W. Deng, C. Yan, T. Yang, X. Chu, G. Tian, D. Xiong, J. Lu, and W. Yang, “Polarization-free high-crystallization β -PVDF piezoelectric nanogenerator toward self-powered 3D acceleration sensor,” *Nano Energy*, vol. 50, pp. 632–638, 2018.
- [130] M. Vilaseca, J. Coronas, A. Cirera, A. Cornet, J. R. Morante, and J. Santamaría, “Use of zeolite films to improve the selectivity of reactive gas sensors,” *Catal. Today*, vol. 82, no. 1, pp. 179–185, 2003.
- [131] N. Li, X. Li, T. Zhang, S. Qiu, G. Zhu, W. Zheng, and W. Yu, “Host–guest composite materials of LiCl/NaY with wide range of humidity sensitivity,” *Mater. Lett.*, vol. 58, no. 10, pp. 1535–1539, 2004.
- [132] M. Urbiztondo, I. Pellejero, A. Rodriguez, M. P. Pina, and J. Santamaria, “Zeolite-coated interdigital capacitors for humidity sensing,” *Sensors Actuators B Chem.*, vol. 157, no. 2, pp. 450–459, 2011.
- [133] E. Coutino-Gonzalez, W. Baekelant, B. Dieu, M. B. J. Roeffaers, and J. Hofkens, “Nanostructured Ag-zeolite Composites as Luminescence-based Humidity Sensors,” *J. Vis. Exp. JoVE*, no. 117, 2016.
- [134] Y. Chen, Y. Zhang, D. Li, F. Gao, C. Feng, S. Wen, and S. Ruan, “Humidity sensor based on AlPO₄-5 zeolite with high responsivity and its sensing mechanism,” *Sensors Actuators B Chem.*, vol. 212, pp. 242–247, 2015.
- [135] W. Zang, Y. Nie, D. Zhu, P. Deng, L. Xing, and X. Xue, “Core–Shell In₂O₃/ZnO Nanoarray Nanogenerator as a Self-Powered Active Gas Sensor with High H₂S

- Sensitivity and Selectivity at Room Temperature,” *J. Phys. Chem. C*, vol. 118, no. 17, pp. 9209–9216, May 2014.
- [136] B. Yu, Y. Fu, P. Wang, Y. Zhao, L. Xing, and X. Xue, “Enhanced piezo-humidity sensing of a Cd–ZnO nanowire nanogenerator as a self-powered/active gas sensor by coupling the piezoelectric screening effect and dopant displacement mechanism,” *Phys. Chem. Chem. Phys.*, vol. 17, no. 16, pp. 10856–10860, 2015.
- [137] W. Zang, W. Wang, D. Zhu, L. Xing, and X. Xue, “Humidity-dependent piezoelectric output of Al–ZnO nanowire nanogenerator and its applications as a self-powered active humidity sensor,” *RSC Adv.*, vol. 4, no. 99, pp. 56211–56215, 2014.
- [138] T. Zhao, Y. Fu, Y. Zhao, L. Xing, and X. Xue, “Ga-doped ZnO nanowire nanogenerator as self-powered/active humidity sensor with high sensitivity and fast response,” *J. Alloys Compd.*, vol. 648, pp. 571–576, 2015.
- [139] D. Zhu, T. Hu, Y. Zhao, W. Zang, L. Xing, and X. Xue, “High-performance self-powered/active humidity sensing of Fe-doped ZnO nanoarray nanogenerator,” *Sensors Actuators B Chem.*, vol. 213, pp. 382–389, 2015.
- [140] Y. Su, G. Xie, S. Wang, H. Tai, Q. Zhang, H. Du, X. Du, and Y. Jiang, “Self-powered humidity sensor based on triboelectric nanogenerator,” in *2017 IEEE SENSORS*, 2017, pp. 1–3.
- [141] H. Guo, J. Chen, L. Tian, Q. Leng, Y. Xi, and C. Hu, “Airflow-Induced Triboelectric Nanogenerator as a Self-Powered Sensor for Detecting Humidity and Airflow Rate,” *ACS Appl. Mater. Interfaces*, vol. 6, no. 19, pp. 17184–17189, Oct. 2014.
- [142] Y. Yu, J.-P. Ma, and Y.-B. Dong, “Luminescent humidity sensors based on porous Ln 3+-MOFs,” *CrystEngComm*, vol. 14, no. 21, pp. 7157–7160, 2012.
- [143] S. Achmann, G. Hagen, J. Kita, I. M. Malkowsky, C. Kiener, and R. Moos, “Metal-organic frameworks for sensing applications in the gas phase,” *Sensors*, vol. 9, no. 3, pp. 1574–1589, 2009.
- [144] R. Grunker, V. Bon, A. Heerwig, N. Klein, P. Müller, U. Stoeck, I. A. Baburin, U. Mueller, I. Senkovska, and S. Kaskel, “Dye Encapsulation Inside a New Mesoporous Metal–Organic Framework for Multifunctional Solvatochromic-Response Function,” *Chem. Eur. J.*, vol. 18, no. 42, pp. 13299–13303, 2012.
- [145] Z. Hu, C. Tao, H. Liu, X. Zou, H. Zhu, and J. Wang, “Fabrication of an NH₂-MIL-88B photonic film for naked-eye sensing of organic vapors,” *J. Mater. Chem. A*, vol. 2, no. 34, pp. 14222–14227, 2014.
- [146] I. Stassen, B. Bueken, H. Reinsch, J. F. M. Oudenhoven, D. Wouters, J. Hajek, V. Van Speybroeck, N. Stock, P. M. Vereecken, and R. Van Schaijk, “Towards metal–organic framework based field effect chemical sensors: UiO-66-NH₂ for nerve agent detection,” *Chem. Sci.*, vol. 7, no. 9, pp. 5827–5832, 2016.
- [147] D. C. Pugh, E. J. Newton, A. J. T. Naik, S. M. V Hailes, and I. P. Parkin, “The gas sensing properties of zeolite modified zinc oxide,” *J. Mater. Chem. A*, vol. 2, no. 13, pp. 4758–

- 4764, 2014.
- [148] Y. Zheng, X. Li, and P. K. Dutta, "Exploitation of unique properties of zeolites in the development of gas sensors," *Sensors*, vol. 12, no. 4, pp. 5170–5194, 2012.
- [149] C. Pijolat, C. Pupier, C. Testud, R. Lalauze, L. Montanaro, A. Negro, and C. Malvicino, "Electrochemical Sensors for CO/NO_x Detection in Automotive Applications," *J. Electroceramics*, vol. 2, no. 3, pp. 181–191, 1998.
- [150] R. Pohle, E. Magori, A. Tawil, P. Davydovskaya, and M. Fleischer, "Detection of NO_x in Combustion Engine Exhaust Gas by Applying the Pulsed Polarization Technique on YSZ Based Sensors," in *Multidisciplinary Digital Publishing Institute Proceedings*, 2017, vol. 1, no. 4, p. 490.
- [151] C. Guardiola, J. Martín, B. Pla, and P. Bares, "Cycle by cycle NO_x model for diesel engine control," *Appl. Therm. Eng.*, vol. 110, pp. 1011–1020, 2017.
- [152] Y. Su, G. Xie, H. Tai, S. Li, B. Yang, S. Wang, Q. Zhang, H. Du, H. Zhang, X. Du, and Y. Jiang, "Self-Powered Room Temperature NO₂ Detection Driven by Triboelectric Nanogenerator under UV illumination," *Nano Energy*.
- [153] C. Kübel, "Automotive Hydrogen Sensors: Current and Future Requirements BT - Solid State Gas Sensors - Industrial Application," M. Fleischer and M. Lehmann, Eds. Berlin, Heidelberg: Springer Berlin Heidelberg, 2012, pp. 35–38.
- [154] A. S. M. I. Uddin and G.-S. Chung, "A self-powered active hydrogen sensor based on a high-performance triboelectric nanogenerator using a wrinkle-micropatterned PDMS film," *RSC Adv.*, vol. 6, no. 67, pp. 63030–63036, 2016.
- [155] S.-H. Shin, Y. H. Kwon, Y.-H. Kim, J.-Y. Jung, and J. Nah, "Triboelectric hydrogen gas sensor with pd functionalized surface," *Nanomaterials*, vol. 6, no. 10, p. 186, 2016.
- [156] A. S. M. I. Uddin and G.-S. Chung, "A self-powered active hydrogen gas sensor with fast response at room temperature based on triboelectric effect," *Sensors Actuators B Chem.*, vol. 231, pp. 601–608, 2016.
- [157] Y. Fu, W. Zang, P. Wang, L. Xing, X. Xue, and Y. Zhang, "Portable room-temperature self-powered/active H₂ sensor driven by human motion through piezoelectric screening effect," *Nano Energy*, vol. 8, pp. 34–43, 2014.
- [158] K. Nam, S. Oh, H. Fujimoto, and Y. Hori, "Estimation of sideslip and roll angles of electric vehicles using lateral tire force sensors through RLS and Kalman filter approaches," *IEEE Trans. Ind. Electron.*, vol. 60, no. 3, pp. 988–1000, 2013.
- [159] X. Gao and Z. Yu, "Vehicle Sideslip Angel Estimation by using High Gain Observer," in *AVEC 9th International Symposium on Advanced Vehicle Control*, 2008, pp. 509–514.
- [160] G. Baffet, A. Charara, and D. Lechner, "Estimation of vehicle sideslip, tire force and wheel cornering stiffness," *Control Eng. Pract.*, vol. 17, no. 11, pp. 1255–1264, 2009.
- [161] Y.-H. J. Hsu, *Estimation and control of lateral tire forces using steering torque*. Stanford University, 2009.

- [162] M. Doumiati, A. C. Victorino, A. Charara, and D. Lechner, "Onboard real-time estimation of vehicle lateral tire-road forces and sideslip angle," *IEEE/ASME Trans. Mechatronics*, vol. 16, no. 4, pp. 601–614, 2011.
- [163] M. Doumiati, A. Victorino, D. Lechner, G. Baffet, and A. Charara, "Observers for vehicle tyre/road forces estimation: experimental validation," *Veh. Syst. Dyn.*, vol. 48, no. 11, pp. 1345–1378, 2010.
- [164] W. Cho, J. Yoon, S. Yim, B. Koo, and K. Yi, "Estimation of tire forces for application to vehicle stability control," *IEEE Trans. Veh. Technol.*, vol. 59, no. 2, pp. 638–649, 2010.
- [165] A. Albinsson, F. Bruzelius, M. Jonasson, and B. Jacobson, "Tire force estimation utilizing wheel torque measurements and validation in simulations and experiments," in *12th International Symposium on Advanced Vehicle Control (AVEC'14), Tokyo Japan, 2014*, pp. 294–299.
- [166] H. Hamann, J. K. Hedrick, S. Rhode, and F. Gauterin, "Tire force estimation for a passenger vehicle with the unscented kalman filter," in *Intelligent Vehicles Symposium Proceedings, 2014 IEEE, 2014*, pp. 814–819.
- [167] E. Hashemi, M. Pirani, A. Khajepour, B. Fidan, A. Kasaiezadeh, S.-K. Chen, and B. Litkouhi, "Integrated estimation structure for the tire friction forces in ground vehicles," in *Advanced Intelligent Mechatronics (AIM), 2016 IEEE International Conference on, 2016*, pp. 1657–1662.
- [168] E. Hashemi, "Full Vehicle State Estimation Using a Holistic Corner-based Approach," 2017.
- [169] E. Hashemi, M. Pirani, A. Khajepour, A. Kasaiezadeh, S.-K. Chen, and B. Litkouhi, "Corner-based estimation of tire forces and vehicle velocities robust to road conditions," *Control Eng. Pract.*, vol. 61, pp. 28–40, 2017.
- [170] J. Yu, J. Chen, Y. Peng, and H. Liu, "Nonlinear observer for longitudinal and lateral velocities of vehicles based on the estimation of longitudinal tire forces," in *American Control Conference (ACC), 2016, 2016*, pp. 6887–6892.
- [171] J. V. Alcantar and F. Assadian, "Longitudinal Tire Force Estimation Using Youla Controller Output Observer," *IEEE Control Syst. Lett.*, vol. 2, no. 1, pp. 31–36, 2018.
- [172] Y. Hu, C. Xu, Y. Zhang, L. Lin, R. L. Snyder, and Z. L. Wang, "A nanogenerator for energy harvesting from a rotating tire and its application as a self-powered pressure/speed sensor," *Adv. Mater.*, vol. 23, no. 35, pp. 4068–71, Sep. 2011.
- [173] H. Zhang, Y. Yang, X. Zhong, Y. Su, Y. Zhou, C. Hu, and Z. L. Wang, "Single-electrode-based rotating triboelectric nanogenerator for harvesting energy from tires," *ACS Nano*, vol. 8, no. 1, pp. 680–689, 2013.
- [174] Y. Mao, D. Geng, E. Liang, and X. Wang, "Single-electrode triboelectric nanogenerator for scavenging friction energy from rolling tires," *Nano Energy*, vol. 15, pp. 227–234, 2015.
- [175] J. Chen, H. Guo, G. Liu, X. Wang, Y. Xi, M. S. Javed, and C. Hu, "A fully-packaged and

- robust hybridized generator for harvesting vertical rotation energy in broad frequency band and building up self-powered wireless systems,” *Nano Energy*, vol. 33, pp. 508–514, 2017.
- [176] T. Guo, G. Liu, Y. Pang, B. Wu, F. Xi, J. Zhao, T. Bu, X. Fu, X. Li, C. Zhang, and Z. L. Wang, “Compressible hexagonal-structured triboelectric nanogenerators for harvesting tire rotation energy,” *Extrem. Mech. Lett.*, vol. 18, pp. 1–8, 2018.
- [177] J. Qian, D.-S. Kim, and D.-W. Lee, “On-vehicle triboelectric nanogenerator enabled self-powered sensor for tire pressure monitoring,” *Nano Energy*, vol. 49, pp. 126–136, 2018.
- [178] H. Askari, E. Hashemi, A. Khajepour, M. B. Khamesee, and Z. L. Wang, “Tire Condition Monitoring and Intelligent Tires Using Nanogenerators Based on Piezoelectric, Electromagnetic, and Triboelectric Effects,” *Adv. Mater. Technol.*, vol. 0, no. 0, p. 1800105, Aug. 2018.
- [179] T. Guo, J. Zhao, W. Liu, G. Liu, Y. Pang, T. Bu, F. Xi, C. Zhang, and X. Li, “Self-Powered Hall Vehicle Sensors Based on Triboelectric Nanogenerators,” *Adv. Mater. Technol.*, vol. 3, no. 8, p. 1800140, 2018.
- [180] L. Zuo, B. Scully, J. Shestani, and Y. Zhou, “Design and characterization of an electromagnetic energy harvester for vehicle suspensions,” *Smart Mater. Struct.*, vol. 19, no. 4, p. 45003, 2010.
- [181] R. Roberto, “Regenerative and Adaptive Shock Absorber: A Hybrid Design,” UWSpace, 2014.
- [182] E. Asadi, R. Ribeiro, M. B. Khamesee, and A. Khajepour, “Analysis, Prototyping, and Experimental Characterization of an Adaptive Hybrid Electromagnetic Damper for Automotive Suspension Systems,” *IEEE Trans. Veh. Technol.*, vol. 66, no. 5, pp. 3703–3713, 2017.
- [183] E. Asadi, “Hybrid Electromagnetic Vibration Isolation Systems,” UWSpace, 2017.

Highlights

- The potential of nanogenerators for self-powered sensing and energy harvesting in automotive systems is discussed.
- A comprehensive review is provided on the current technologies in automotive sensing.
- A list of sensors and devices which can be improved to self-powered category in automotive systems using nanogenerators are presented.
- Five different categories of sensors in automotive systems are reviewed.